The Stability of Steady-State Hot-Spot Patterns for a Reaction-Diffusion Model of Urban Crime

T. KOLOKOLNIKOV, M. J. WARD, and J. WEI

Theodore Kolokolnikov; Department of Mathematics, Dalhousie University, Halifax, Nova Scotia, B3H 3J5, Canada,
Michael Ward; Department of Mathematics, University of British Columbia, Vancouver, British Columbia, V6T 1Z2, Canada,
Juncheng Wei, Department of Mathematics, Chinese University of Hong Kong, Shatin, New Territories, Hong Kong.

(*Received December 22, 2011*)

The existence and stability of localized patterns of criminal activity are studied for the reaction-diffusion model of urban crime that was introduced by Short et. al. [Math. Models. Meth. Appl. Sci., **18**, Suppl. (2008), pp. 1249–1267]. Such patterns, characterized by the concentration of criminal activity in localized spatial regions, are referred to as hot-spot patterns and they occur in a parameter regime far from the Turing point associated with the bifurcation of spatially uniform solutions. Singular perturbation techniques are used to construct steady-state hot-spot patterns in one and two-dimensional spatial domains, and new types of nonlocal eigenvalue problems are derived that determine the stability of these hot-spot patterns to $\mathcal{O}(1)$ time-scale instabilities. From an analysis of these nonlocal eigenvalue problems, a critical threshold K_c is determined such that a pattern consisting of K hot-spots is unstable to a competition instability if $K > K_c$. This instability, due to a positive real eigenvalue, triggers the collapse of some of the hot-spots in the pattern. Furthermore, in contrast to the well-known stability results for spike patterns of the Gierer-Meinhardt reaction-diffusion model, it is shown for the crime model that there is only a relatively narrow parameter range where oscillatory instabilities in the hot-spot amplitudes occur. Such an instability, due to a Hopf bifurcation, is studied explicitly for a single hot-spot in the shadow system limit, for which the diffusivity of criminals is asymptotically large. Finally, the parameter regime where localized hot-spots occur is compared with the parameter regime, studied in previous works, where Turing instabilities from a spatially uniform steady-state occur.

Key words: singular perturbations, hot-spots, reaction-diffusion, crime, nonlocal eigenvalue problem, Hopf Bifurcation.

1 Introduction

Recently, Short *et. al.* [**29**, **30**, **31**] introduced an agent-based model of urban crime that takes into account repeat or near-repeat victimization. In dimensionless form, the continuum limit of this agent-based model is the two-component reaction-diffusion PDE system

$$A_t = \varepsilon^2 \Delta A - A + PA + \alpha\,, \qquad x \in \Omega\,; \qquad \partial_n A = 0\,, \qquad x \in \partial\Omega\,, \tag{1.1 a}$$

$$\tau P_t = D\nabla \cdot \left(\nabla P - \frac{2P}{A} \nabla A \right) - PA + \gamma - \alpha\,, \qquad x \in \Omega\,; \qquad \partial_n P = 0\,, \qquad x \in \partial\Omega\,, \tag{1.1 b}$$

where the positive constants ε^2, D, α, γ and τ, are all assumed to be spatially independent. In this model, $P(x,t)$ represents the density of the criminals, $A(x,t)$ represents the "attractiveness" of the environment to burglary or other criminal activity, and the chemotactic drift term $-2D\nabla \cdot \left(P \frac{\nabla A}{A}\right)$ represents the tendency of criminals to move towards sites with a higher attractiveness. In addition, α is the baseline attractiveness, while $(\gamma - \alpha)/\tau$ represents the constant rate of re-introduction of criminals after a burglary. For further details on the model see [**29**].

In [**29**], the reaction-diffusion system (1.1) with chemotactic drift term was derived from a continuum limit of a lattice-based model. It was then analyzed using linear stability theory to determine a parameter range for the

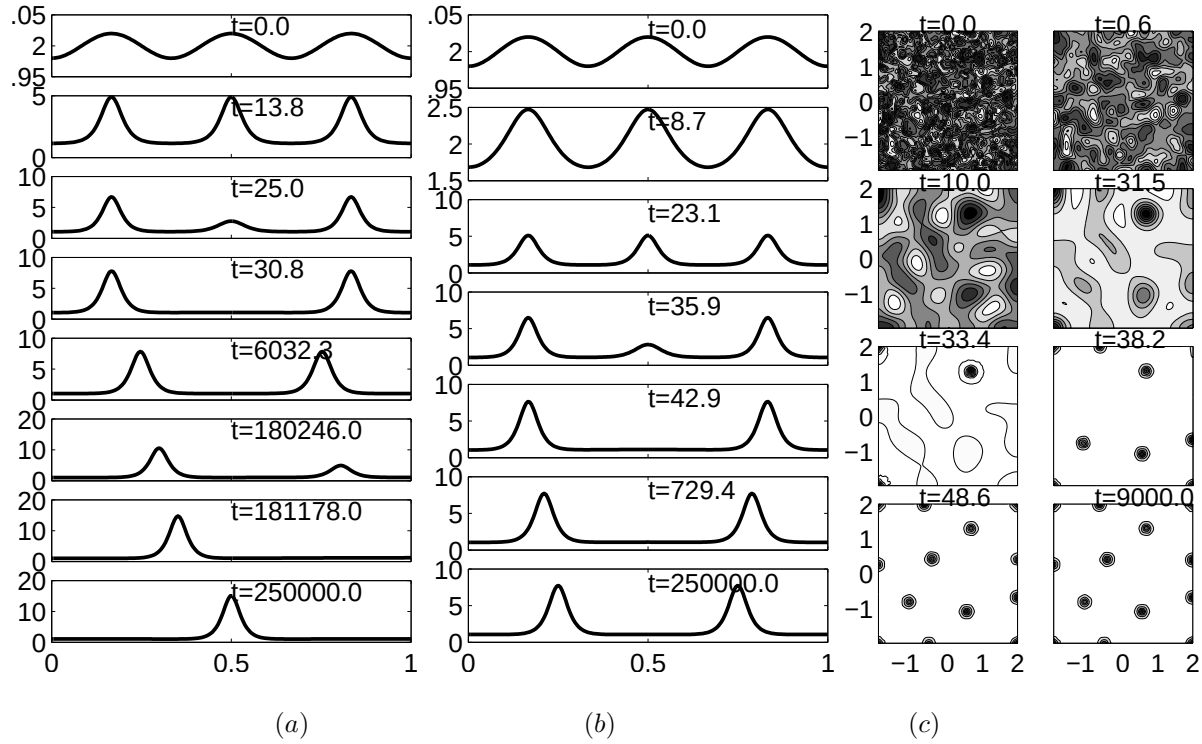

(a) (b) (c)

Figure 1. Numerical solution of (1.1) at different times, for initial data close to a spatially homogeneous steady-state. Plots of $A(x,t)$ are shown at the values of t indicated. (a) One dimensional domain with parameter values $\alpha = 1$, $\gamma = 2$, $\varepsilon = 0.02$, $\tau = 1$, $D = 1$. Initial conditions are $P(x,0) = 1 - \alpha/\gamma$ and $A(x,0) = \gamma(1 - 0.01\cos(6\pi x))$. Turing instability leads to a formation of three hot-spots; one is annihilated almost immediately due to a fast-time instability, while the second hot-spot is annihilated after a long time. (b) $D = 0.5$ with all other parameters as in (a). Two hot-spots remain stable. (c) Numerical solution of (1.1) in a two-dimensional square of width 4. Parameters are $\alpha = 1$, $\gamma = 2$, $\varepsilon = 0.08$, $\tau = 1$, $D = 1$. Initial conditions are $P(x,0) = 1 - \alpha/\gamma$ and $A(x,0) = \gamma(1 + \text{rand} * 0.001)$ where rand generates a random number between 0 and 1.

existence of a Turing instability of the spatially uniform steady-state. A weakly nonlinear theory, based on a multi-scale expansion valid near the Turing bifurcation point, was developed in [**30**, **31**] for (1.1) for both one and two-dimensional domains. This theoretical framework is very useful to explore the origins of various patterns that are observed in full numerical solutions of the model. However, the major drawback of a weakly nonlinear theory is that the parameters must be tuned near the bifurcation point of the Turing instability. When the parameters values are at an $\mathcal{O}(1)$ distance from the bifurcation point, an instability of the spatially homogeneous steady-state often leads to patterns consisting of *localized structures*. Such localized patterns for the crime model (1.1), consisting of the concentration of criminal activity in localized spatial regions, are referred to as either hot-spot or spike-type patterns. A localized hot-spot solution, not amenable to an analytical description by a weakly nonlinear analysis, was observed in the full numerical solutions of [**30**].

As an illustration of localization behavior, in Fig. 1(a) we plot the numerical solution to (1.1) in the one-dimensional domain $\Omega = [0,1]$ with parameter values $\alpha = 1$, $\gamma = 2$, $\varepsilon = 0.02$, $\tau = 1$, and $D = 1$. The initial conditions, consisting of a small mode-three perturbation of the spatially homogeneous steady-state $A_e = \gamma$ and $P_e = (\gamma - \alpha)/\gamma$ are first amplified due to linear instability. Shortly thereafter, nonlinear effects become significant and the solution quickly

becomes localized leading to the formation of three hot-spots, as shown at $t \approx 14$. Subsequently, one of the hot-spots appears to be unstable and is quickly annihilated. The remaining two hot-spots drift towards each other over a long time, until finally around $t \approx 180,000$, another hot-spot is annihilated. The lone remaining hot-spot then drifts towards the center of the domain where it then remains. Next, in Fig. 1(b) we re-run the simulation when D is decreased to $D = 0.5$ with all other parameters the same as in Fig. 1(a). For this value of D, we observe that the final state consists of *two* hot-spots. Similar complex dynamics of hot-spots in a two-dimensional domain are shown in Fig. 1(c).

It is the goal of this paper to give a detailed study of the existence and stability of steady-state localized hot-spot patterns for (1.1) in both one and two-dimensional domains in the singularly perturbed limit

$$\varepsilon^2 \ll D\,. \tag{1.2}$$

The assumption that $\varepsilon^2 \ll D$ implies that the length-scale associated with the change in the attractiveness of potential burglary sites is much smaller than the length-scale over which criminals explore new territory to commit crime. In this limit, a singular perturbation methodology will be used to construct steady-state hot-spot solutions and to derive new nonlocal eigenvalue problems (NLEP's) governing the stability of these solutions. From an analysis of the spectrum of these NLEP's, explicit stability thresholds in terms of D and τ for the initiation of $\mathcal{O}(1)$ time-scale instabilities of these patterns are obtained. In a one-dimensional domain, an additional stability threshold on D for the initiation of slow translational instabilities of the hot-spot pattern is derived. Among other results, we will be able to explain both the fast and slow instabilities of the localized hot-spots patterns as observed in Fig. 1(a).

In related contexts, there is now a rather large literature on the stability of spike-type patterns in two-component reaction-diffusion systems with no drift terms. The theory was first developed in a one-dimensional domain to analyze the stability of steady-state spike patterns for the Gierer-Meinhardt model (cf. [**10**, **3**, **35**, **37**, **38**, **34**, **43**, **46**]) and, in a parallel development, the Gray-Scott model (cf. [**4**, **5**, **15**, **23**, **24**, **18**, **1**]). The stability theory for these two models was extended to two-dimensional domains in [**39**, **41**, **40**, **44**, **43**, **2**]. Related studies for the Schnakenburg model are given in [**11**, **36**, **42**]. The dynamics of quasi-equilibrium spike patterns is studied for one-dimensional domains in [**9**, **6**, **7**, **33**, **22**], and in a multi-dimensional context in [**13**, **14**, **16**, **2**]. More recently, in [**19**] the stability of spikes was analyzed for a reaction-diffusion model of species segregation with cross-diffusion. A common feature in all of these studies, is that an analysis of the spectrum of various classes of NLEP's is central for determining the stability properties of localized patterns. A survey of NLEP theory is given in [**46**], and in, a broader context, a survey of phenomena and results for far-from-equilibrium patterns is given in [**25**].

In contrast, for reaction-diffusion systems with chemotactic drift terms, such as the crime model (1.1), there are only a few studies of the existence and stability of spike solutions. These previous studies have focused mainly on variants of the well-known Keller-Segel model (cf. [**8**, **12**, **28**, **32**]).

We now summarize and illustrate our main results. In §2.1 we construct a multi hot-spot steady state solution to (1.1) on a one-dimensional interval of length S. We refer to a symmetric hot-spot steady-state solution as one for which the hot-spots are equally spaced and, correspondingly, each hot-spot has the same amplitude. In §2.2 asymmetric steady-state hot-spot solutions, characterized by unevenly spaced hot-spots, are shown to bifurcate from the symmetric branch of hot-spot solutions at a critical value of D.

In §3 we study the stability of steady-state K-hot-spot solutions on an interval of length S when $\tau = \mathcal{O}(1)$. A singular perturbation approach is used to derive a NLEP that determines the stability of these hot-spot patterns to

$\mathcal{O}(1)$ time-scale instabilities. In contrast to the NLEP's arising in the study of spike stability for the Gierer-Meinhardt model (cf. [**35**]), this NLEP is explicitly solvable. In this way, a critical threshold K_{c+} is determined such that a pattern consisting of K hot-spots with $K > 1$ is unstable to a competition instability if and only if $K > K_{c+}$. This instability, which develops on an $\mathcal{O}(1)$ time scale as $\varepsilon \to 0$, is due to a positive real eigenvalue, and it triggers the collapse of some of the hot-spots in the pattern. This critical threshold $K_{c+} > 0$ is the unique root of (see Principal Result 3.2 below)

$$K\left(1+\cos\left(\pi/K\right)\right)^{1/4} = \left(\frac{S}{2}\right)\left(\frac{2}{D}\right)^{1/4}\frac{(\gamma-\alpha)^{3/4}}{\sqrt{\pi\varepsilon\alpha}}\,. \tag{1.3}$$

In addition, from the location of the bifurcation point associated with the birth of an asymmetric hot-spot equilibrium, a further threshold K_{c-} is derived that predicts that a K-hot-spot steady-state with $K > 1$ is stable with respect to slow translational instabilities of the hot-spot locations if and only if $K < K_{c-}$. This threshold is given explicitly by (see (3.20) below)

$$K_{c-} = \left(\frac{S}{2}\right)D^{-1/4}\frac{(\gamma-\alpha)^{3/4}}{\sqrt{\pi\varepsilon\alpha}}\,. \tag{1.4}$$

Since $K_{c-} < K_{c+}$, the stability properties of a K-hot-spot steady-state solution with $K > 1$ and $\tau = \mathcal{O}(1)$ are as follows: stability when $K < K_{c-}$; stability with respect to $\mathcal{O}(1)$ time-scale instabilities but unstable with respect to slow translation instabilities when $K_{c-} < K < K_{c+}$; a fast $\mathcal{O}(1)$ time-scale instability dominates when $K > K_{c+}$.

As an illustration of these results consider again Fig. 1(a). From the parameter values in the figure caption we compute from (1.3) and (1.4) that $K_{c+} \approx 2.273$ and $K_{c-} \approx 1.995$. Therefore, we predict that the three hot-spots that form at $t = 13.8$ are unstable on an $\mathcal{O}(1)$ time-scale. This is confirmed by the numerical results shown at times $t = 25$ and $t = 30.8$ in Fig. 1(a). We then predict from the threshold K_{c-} that the two-hot-spot solution will become unstable on a very long time interval. This is also confirmed by the full numerical solutions shown in Fig. 1(a). In contrast, if we decrease D to $D = 0.5$ as in Fig. 1(b) then we calculate from (1.3) and (1.4) that $K_{c+} \approx 2.612$ and $K_{c-} \approx 2.372$. Our prediction is that the three hot-spot solution that emerges from initial data will be unstable on an $\mathcal{O}(1)$ time-scale, but that a two-hot-spot steady-state will be stable. These predictions are again corroborated by the full numerical results.

In §4 we examine oscillatory instabilities of the amplitudes of the hot-spots in terms of the bifurcation parameter τ in (1.1). From an analysis of a new NLEP with two separate nonlocal terms, we show that an oscillatory instability of the hot-spot amplitudes as a result of a Hopf bifurcation is not possible on the regime $\tau \leq \mathcal{O}(\varepsilon^{-1})$. This non-existence result for a Hopf bifurcation is in contrast to the results obtained in [**35**] for the Gierer-Meinhardt model showing the existence of oscillatory instabilities of the spike amplitudes in a rather wide parameter regime. However, for the asymptotically larger range of τ with $\tau = \mathcal{O}(\varepsilon^{-2})$, in §4.1 we study oscillatory instabilities of a single hot-spot in the simplified system corresponding to letting $D \to \infty$ in (1.1). In this shadow system limit, we show for a domain of length one that low frequency oscillations of the spot amplitude due to a Hopf bifurcation will occur when $\tau > \tau_c$ where

$$\tau_c \sim 0.039759(\gamma-\alpha)^3\alpha^{-2}\varepsilon^{-2}\,.$$

In §5 we extend our results to two dimensional domains. We first construct a quasi-equilibrium multi hot-spot pattern, and then derive an NLEP governing $\mathcal{O}(1)$ time-scale instabilities of the spot pattern. As in the analyses of [**39**, **40**, **41**, **42**, **43**, **44**] for the Gierer-Meinhardt and Gray-Scott models, our existence and stability theory for localized hot-spot solutions is accurate only to leading-order in powers of $-1/\log\varepsilon$. In §5.1, we show from an analysis

of a certain NLEP problem that for $\tau = \mathcal{O}(1)$ a K-hot-spot solution with $K > 1$ is unstable when $K > K_c$ where

$$K_c \sim \frac{D^{-1/3}|\Omega|(\gamma-\alpha)\alpha^{-2/3}}{\left[4\pi\left(\int_{\mathbb{R}^2} w^3\,dy\right)^2\right]^{1/3}}\varepsilon^{-4/3}\left(-\log\varepsilon\right)^{1/3} \approx (0.07037)\; D^{-1/3}\alpha^{-2/3}\left(\gamma-\alpha\right)|\Omega|\varepsilon^{-4/3}\left(-\log\varepsilon\right)^{1/3}\,, \tag{1.5}$$

as $\varepsilon \to 0$. Here w is the radially symmetric ground-state solution of $\Delta w - w + w^3 = 0$ in $\mathbb{R}^2$ and $|\Omega|$ is the area of Ω. As an example, consider the parameter values as in Fig. 1(c), for which $|\Omega| = 16$. Then, from (1.5) we get $K_c \approx 44.48$. Starting with random initial conditions, we observe from Fig. 1(c) that at $t = 9000$ we have $K = 7.5$ hot-spots, where we count boundary spots having weight $1/2$ and corner spots having weight $1/4$. Since $K < K_c$, this is in agreement with the stability theory.

Finally, in §5, we contrast results for Turing instabilities and Turing patterns with our results for localized hot-spots. We also propose a few open problems.

2 Asymptotic Analysis of Steady-State Hot-Spot Solutions in 1-D

In the 1-D interval $x \in [-l, l]$, the reaction-diffusion system (1.1) is

$$A_t = \varepsilon^2 A_{xx} - A + PA + \alpha \tag{2.1 a}$$

$$\tau P_t = D\left(P_x - \frac{2P}{A}A_x\right)_x - PA + \gamma - \alpha\,, \tag{2.1 b}$$

with Neumann boundary conditions $P_x(\pm l, t) = A_x(\pm l, t) = 0$. Since $P_x - \frac{2P}{A}A_x = (P/A^2)_x A^2$, it is convenient to introduce the new variable V defined by

$$V = P/A^2\,, \tag{2.2}$$

so that (2.1) transforms to

$$A_t = \varepsilon^2 A_{xx} - A + VA^3 + \alpha\,, \tag{2.3 a}$$

$$\tau\left(A^2 V\right)_t = D\left(A^2 V_x\right)_x - VA^3 + \gamma - \alpha\,. \tag{2.3 b}$$

To motivate the ε-dependent re-scaling of V that facilitates the analysis below, we suppose that $D \gg l^2$ and we integrate the steady-state of (2.3 b) over $-l < x < l$ to obtain that $V = c/\int_{-l}^{l} A^3\,dx$, where c is some $\mathcal{O}(1)$ constant as $\varepsilon \to 0$. Therefore, if $A = \mathcal{O}(\varepsilon^{-p})$ in the inner hot-spot region of spatial extent $\mathcal{O}(\varepsilon)$, we conclude that $\int_{-l}^{l} A^3\,dx = \mathcal{O}(\varepsilon^{1-3p})$, so that $V = \mathcal{O}(\varepsilon^{3p-1})$. In addition, from the steady-state of (2.3 a), we conclude that in the inner region near a hot-spot centered at $x = x_0$ we must have $-A + A^3 V = \mathcal{O}(A_{yy})$, where $y = (x - x_0)/\varepsilon$ and $A = \mathcal{O}(\varepsilon^{-p})$. This implies that $-3p + (3p-1) = -p$, so that $p = 1$. Therefore, for $D \gg l^2$ we conclude that $V = \mathcal{O}(\varepsilon^2)$ globally on $-l < x < l$, while $A = \mathcal{O}(\varepsilon^{-1})$ in the inner region near a hot-spot. Finally, in the outer region we must have $A = \mathcal{O}(1)$, so that from the steady-state of (2.3 b), we conclude that $D\left(A^2 V_x\right)_x \sim \alpha - \gamma = \mathcal{O}(1)$. Since $V = \mathcal{O}(\varepsilon^2)$, this balance requires that $D = \mathcal{O}(\varepsilon^{-2})$. Since $V = \mathcal{O}(\varepsilon^2)$ globally, while $A = \mathcal{O}(\varepsilon^{-1})$ in the core of a hot-spot, we conclude that within a hot-spot of criminal activity the density $P = VA^2$ of criminals is $\mathcal{O}(1)$.

In summary, this simple scaling analysis motivates the introduction of new $\mathcal{O}(1)$ variables v and D_0 defined by

$$V = \varepsilon^2 v\,, \qquad D = D_0/\varepsilon^2\,. \tag{2.4}$$

In terms of (2.4), (2.3) transforms to

$$A_t = \varepsilon^2 A_{xx} - A + \varepsilon^2 v A^3 + \alpha\,, \qquad -l < x < l\,; \qquad A_x(\pm l, t) = 0\,, \tag{2.5 a}$$

$$\tau\varepsilon^2 \left(A^2 v\right)_t = D_0 \left(A^2 v_x\right)_x - \varepsilon^2 v A^3 + \gamma - \alpha\,, \qquad -l < x < l\,; \qquad v_x(\pm l, t) = 0\,. \tag{2.5 b}$$

2.1 A Single Steady-State Hot-Spot Solution

We will now construct a steady-state hot-spot solution on the interval $-l < x < l$ with a peak at the origin. In order to construct a K-hot-spot pattern on a domain of length S, with evenly spaced spots, we need only set $l = S/(2K)$ and perform a periodic extension of the results obtained below on the basic interval $-l < x < l$. As such, the fundamental problem considered below is to asymptotically construct a one-hot-spot steady-state solution on $-l < x < l$.

In the inner region, near the center of the hot-spot at $x = 0$, we expand A and v as

$$A = \frac{A_0}{\varepsilon} + A_1 + \cdots\,, \qquad v = v_0 + \varepsilon v_1 + \cdots\,, \qquad y = x/\varepsilon\,. \tag{2.6}$$

From (2.5 a) we obtain, in terms of y, that $A_j(y)$ for $j = 0, 1$ satisfy

$$A_0'' - A_0 + v_0 A_0^3 = 0\,, \quad -\infty < y < \infty\,, \tag{2.7 a}$$

$$A_1'' - A_1 + +3A_0^2 A_1 v_0 = -\alpha - v_1 A_0^3\,, \quad -\infty < y < \infty\,. \tag{2.7 b}$$

In contrast, from (2.5 b), we obtain that v_j for $j = 0, 1$ satisfy

$$\left(A_0^2 v_0'\right)' = 0\,, \qquad \left(A_0^2 v_1' + 2A_0 A_1' v_0'\right)' = 0\,, \qquad -\infty < y < \infty\,. \tag{2.8}$$

In order to match to an outer solution, we require that v_0 and v_1 are bounded as $|y| \to \infty$. In this way, we then obtain that v_0 and v_1 must both be constants, independent of y.

We look for a solution to (2.7) for which the hot-spot has a maximum at $y = 0$. The homoclinic solution to (2.7 a) with $A_0'(0) = 0$ is written as

$$A_0(y) = v_0^{-1/2} w(y)\,, \tag{2.9}$$

where w is the unique solution to the ground-state problem

$$w'' - w + w^3 = 0\,, \quad -\infty < y < \infty\,; \quad w(0) > 0\,, \quad w'(0) = 0\,; \quad w \to 0 \quad \text{as} \quad |y| \to \infty\,, \tag{2.10}$$

given explicitly by $w = \sqrt{2}\,\mathrm{sech}\, y$. Next, we decompose the solution A_1 to (2.7 b) as

$$A_1 = \alpha - \frac{v_1}{2v_0^{3/2}} w - 3\alpha w_1\,,$$

where $w_1(y)$ satisfies

$$L_0 w_1 \equiv w_1'' - w_1 + 3w^2 w_1 = w^2\,, \qquad -\infty < y < \infty\,, \tag{2.11}$$

with $w_1'(0) = 0$ and $w_1 \to 0$ as $|y| \to \infty$.

A key property of the operator L_0, which relies on the cubic exponent in (2.10), is the remarkable identity that

$$L_0 w^2 = 3w^2\,. \tag{2.12}$$

The proof of this identity is a straightforward manipulation of (2.10) and the operator L_0 in (2.11). This property

plays an important role in an explicit analysis of the spectral problem in §3. Here this identity is used to provide an explicit solution to (2.11) in the form

$$w_1 = w^2/3\,.$$

In this way, in the inner region the two-term expansion for A in terms of the unknown constants v_0 and v_1 is

$$A(y) \sim \varepsilon^{-1}A_0(y) + A_1(y) + \cdots\,, \qquad A_0(y) = \varepsilon^{-1}v_0^{-1/2}w(y)\,, \qquad A_1(y) = \alpha\left(1 - [w(y)]^2\right) - \frac{v_1}{2v_0^{3/2}}w(y)\,. \tag{2.13}$$

In the outer region, defined for $\varepsilon \ll |x| \le l$, we have that $v = \mathcal{O}(1)$ and that $A = \mathcal{O}(1)$. From (2.5), we obtain that

$$A = \alpha + o(1)\,, \qquad v = h_0(x) + o(1)\,,$$

where from (2.5 b), $h_0(x)$ satisfies

$$h_{0xx} = \zeta \equiv \frac{(\alpha-\gamma)}{D_0\alpha^2} < 0\,, \qquad 0 < |x| \le l\,; \qquad h_{0x}(\pm l) = 0\,,$$

subject to the matching condition that $h_0 \to v_0$ as $x \to 0^{\pm}$. The solution to this problem gives the outer expansion

$$v \sim h_0(x) = \frac{\zeta}{2}\left[(l-|x|)^2 - l^2\right] + v_0\,, \qquad 0 < |x| \le l\,. \tag{2.14}$$

Next, we must calculate the constants v_0 and v_1 appearing in (2.13) and (2.14). We integrate (2.5 b) over $-l < x < l$ and use $v_x = 0$ at $x = \pm l$ to get

$$\varepsilon^2\int_{-l}^{l} vA^3\,dx = 2l(\alpha-\gamma)\,.$$

Since $A = \mathcal{O}(\varepsilon^{-1})$ in the inner region, while $A = \mathcal{O}(1)$ in the outer region, the dominant contribution to the integral in (2.1) arises from the inner region where $x = \mathcal{O}(\varepsilon)$. If we use the inner expansion $A = \varepsilon^{-1}A_0 + A_1 + o(1)$ from (2.13), and change variables to $y = \varepsilon^{-1}x$, we obtain from (2.1) that

$$v_0\int_{-\infty}^{\infty} A_0^3\,dy + \varepsilon\left(3v_0\int_{-\infty}^{\infty} A_0^2A_1\,dy + v_1\int_{-\infty}^{\infty} A_0^3\right) + \mathcal{O}(\varepsilon^2) = 2l(\alpha-\gamma)\,. \tag{2.15}$$

In (2.15), we emphasize that the first two terms on the left-hand side arise solely from the inner expansion, whereas the $\mathcal{O}(\varepsilon^2)$ term would be obtained from both the inner and outer expansions. By equating coefficients of ε in (2.15), we obtain that

$$v_0 = 2l(\gamma-\alpha)/\int_{-\infty}^{\infty} A_0^3\,dy\,, \qquad v_1 = -3v_0\int_{-\infty}^{\infty} A_0^2A_1\,dy/\int_{-\infty}^{\infty} A_0^3\,dy\,,$$

Then, upon using (2.13) for A_0 and A_1, together with $w = \sqrt{2}\,\mathrm{sech}\,y$, $\int_{-\infty}^{\infty} w^3\,dy = \sqrt{2}\pi$, and $\int_{-\infty}^{\infty} w^4\,dy = 16/3$, we readily derive from (2.1) that

$$v_0 = \frac{\pi^2}{2l^2\,(\alpha-\gamma)^2}\,, \qquad v_1 = 6v_0^{3/2}\alpha\left(\frac{\int_{-\infty}^{\infty}\left(w^2-w^4\right)\,dy}{\int_{-\infty}^{\infty} w^3\,dy}\right) = -\frac{4\sqrt{2}}{\pi}v_0^{3/2}\alpha = -\frac{2\alpha\pi^2}{l^3(\gamma-\alpha)^3}\,. \tag{2.16}$$

We summarize our result for a single steady-state hot-spot solution as follows:

Principal Result 2.1: *Let $\varepsilon \to 0$, and consider a one-hot-spot solution centered at the origin for (2.5) on the interval $|x| \le l$. Then, in the inner region $y = x/\varepsilon = \mathcal{O}(1)$, we have*

$$A(y) = \frac{w}{\varepsilon\sqrt{v_0}} + \alpha\left(1 + \frac{2\sqrt{2}}{\pi}w - w^2\right) + o(1)\,, \qquad v \sim v_0 + \varepsilon v_1 + \cdots\,. \tag{2.17}$$

In addition, in the inner region, the leading-order steady-state criminal density P from (2.1) is $P \sim w^2$. Here $w =$

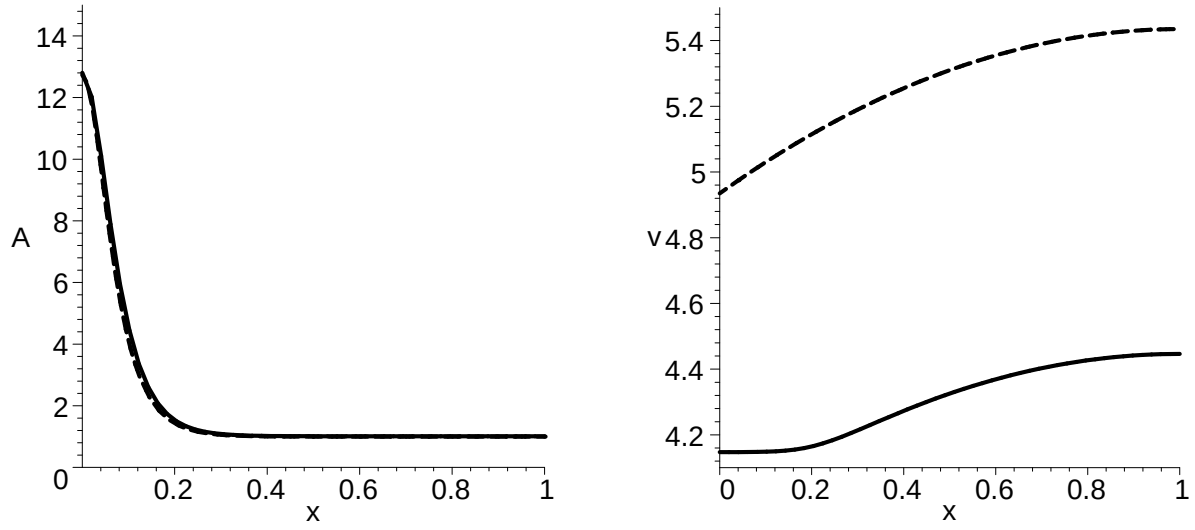

(a) (b)

Figure 2. Steady-state solution in one spatial dimension. Parameter values are $D_0 = 1, \varepsilon = 0.05, \alpha = 1, \gamma = 2$, and $x \in [0, 1]$. (a) The solid line is the steady state solution $A(x)$ of (2.5) computed by solving the boundary value problem numerically. The dashed line corresponds to the first-order composite approximation given by (2.19) (b) The solid line is the steady state solution for $v(x)$. Note the "flat knee" region obtained from the full numerical solution in the inner region near the center of the hot-spot. The dashed line is the leading-order asymptotic result (2.18).

ε	$A(0)$ (num)	$A(0)$ (asy1)	$A(0)$ (asy2)	$v(0)$ (num)	$v(0)$ (asy1)	$v(0)$ (asy2)
0.1	6.281	6.366	6.003	3.5844	4.935	2.961
0.05	12.805	12.732	12.369	4.1474	4.935	3.948
0.025	25.628	25.465	25.101	4.4993	4.935	4.441
0.0125	51.145	50.930	50.566	4.7039	4.935	4.688

Table 1. Comparison of numerical and asymptotic results for the amplitude $A_{\max} \equiv A(0)$ and for $v(0)$ of a one-hot-spot solution on $[-1, 1]$ with $D_0 = 1$, $\gamma = 1$, and $\alpha = 2$. The 1-term and 2-term asymptotic results for $A_{\max}$ and $v(0)$ are obtained from (2.17).

$w(y) = \sqrt{2}\operatorname{sech} y$ is the homoclinic of (2.10), while v_0 and v_1 are given in (2.16). In the outer region, $\mathcal{O}(\varepsilon) < |x| \le l$, then

$$A \sim \alpha + o(1)\,; \qquad v \sim \frac{\zeta}{2}\left((l - |x|)^2 - l^2\right) + v_0 + o(1)\,, \qquad \zeta \equiv \frac{(\alpha - \gamma)}{D_0 \alpha^2} < 0\,. \tag{2.18}$$

Note that to get a solution for A which is uniformly valid in both inner and outer region, we can combine the formulas (2.17) and (2.18). The resulting first-order composite solution is given explicitly by

$$A \sim \left(\frac{2l(\gamma - \alpha)}{\pi\varepsilon} - \alpha\right) \operatorname{sech}\left(\frac{x}{\varepsilon}\right) + \alpha\,. \tag{2.19}$$

For a specific parameter set, a comparison of the full numerical steady-state solution of (2.5) with the composite asymptotic solution (2.19) is shown in Fig. 2. A comparison of numerical and asymptotic values for $A(0)$ and $v(0)$ at various ε is shown in Table 1. From this table we note that the two-term asymptotic expansion for $v(0)$ agrees very favorably with full numerical results.

2.2 Asymmetric Steady-State K-Hot-Spot Solutions

In the limit $\varepsilon \to 0$, we now construct an asymmetric steady-state K-hot-spot solution to (2.5) in the form of a sequence of hot-spots of different heights. This construction will be used to characterize the stability of symmetric steady-state K-hot-spot solutions with respect to the small eigenvalues $\lambda = o(1)$ in the spectrum of the linearization. Since the asymmetric solution is shown to bifurcate from the symmetric branch, the point of the bifurcation corresponds to a zero eigenvalue crossing along the symmetric branch. To determine this bifurcation point, we compute $v(l)$ for the one-hot-spot steady-state solution to (2.5) on $|x| \le l$, where $l > 0$ is a parameter. This canonical problem is shown to have two different solutions. A K-hot-spot asymmetric solution to (2.5) is then obtained by using translates of these two local solutions in such a way to ensure that the resulting solution is C^1 continuous. Since the details of the construction of the asymmetric solution is very similar to that in [**36**] for the Schnakenburg model, we will only give a brief outline of the analysis.

The key quantity of interest is the critical value $D_{0\mathrm{K}}^s$ of D for which an asymmetric K-hot-spot solution branch bifurcates off of the symmetric branch. To this end, we first calculate from (2.14) that

$$v(l) = \frac{(\gamma-\alpha)}{2\alpha^2\sqrt{D_0}} B\left(l/q\right) , \qquad q \equiv \left(\frac{D_0\pi^2\alpha^2}{(\gamma-\alpha)^3}\right)^{1/4} , \tag{2.20 a}$$

where the function $B(z)$ on $0 < z < \infty$ is defined by

$$B(z) \equiv z^2 + 1/z^2 . \tag{2.20 b}$$

The function $B(z) > 0$ in (2.20 *b*) has a unique global minimum point at $z = z_c = 1$, and it satisfies $B^{'}(z) < 0$ on $[0, z_c)$ and $B'(z) > 0$ on (z_c, ∞). Therefore, given any $z \in (0, z_c)$, there exists a unique point $\tilde{z} \in (z_c, \infty)$ such that $B(z) = B(\tilde{z})$. This shows that given any l, with $l/q < z_c = 1$, there exists a unique $\tilde{l}$, with $\tilde{l}/q \equiv \tilde{z} > z_c = 1$, such that $v(l) = v(\tilde{l})$.

We refer to solutions of length l and $\tilde{l}$ as A-type and B-type hot-spots. Now consider the interval $x \in [a, b]$ with length $S \equiv b - a$. To construct a K-hot-spot steady-state solution to (2.5) on this interval with $K_1 \ge 0$ hot-spots of type A and $K_2 = K - K_1 \ge 0$ hot-spots of type B, arranged in any order across the interval, we must solve the coupled system $2K_1 l + 2K_2\tilde{l} = S$ and $B(l/q) = B(\tilde{l}/q)$ for $l \neq \tilde{l}$. Such solution exists only if $l/q < z_c$ and $\tilde{l}/q > z_c$ with $z_c = 1$. The bifurcation point corresponds to the minimum point where $l = \tilde{l} = q$. With $D = D_0/\varepsilon^2$, this yields that

$$l = \left(\frac{D_0\pi^2\alpha^2}{(\gamma-\alpha)^3}\right)^{1/4} = \varepsilon^{1/2}\left(\frac{D\pi^2\alpha^2}{(\gamma-\alpha)^3}\right)^{1/4} . \tag{2.21}$$

At this value of the parameters, a steady-state K-hot-spot asymmetric solution branch bifurcates off of the symmetric K-hot-spot branch. This critical value of D_0 determines the small eigenvalue stability threshold in the linearization of the symmetric K-hot-spot steady-state solution. For a symmetric configuration of K hot-spots on an interval of length S we have $2Kl = S$ so that the critical value $D_0 = D_{0K}^S$, as defined by (2.21), can be written as

$$D_{0K}^S = \frac{(\gamma-\alpha)^3}{\pi^2\alpha^2}\left(\frac{S}{2K}\right)^4 . \tag{2.22}$$

A more detailed construction of the asymmetric solution branches parallels that done in [**36**] for the Schnakenburg model and is left to the reader.

3 The NLEP Stability of Steady-State 1-D Hot-Spot Patterns

We now study the stability of the K-hot-spot steady-state solution to (2.5) that was constructed in §2. The analysis for the "large" $\mathcal{O}(1)$ eigenvalues in the spectrum of the linearization is done in several distinct steps.

Firstly, we let A_e, v_e denote the one-hot-spot quasi-steady-state solution to (2.5) on the basic interval $|x| \le l$, which was given in Principal Result 2.1. Upon introducing the perturbation

$$A = A_e + \phi e^{\lambda t}\,, \qquad v = v_e + \psi e^{\lambda t}\,, \tag{3.1}$$

we obtain from the linearization of (2.5) that

$$\varepsilon^2\phi_{xx} - \phi + 3\varepsilon^2 v_e A_e^2\phi + \varepsilon^3 A_e^3\psi = \lambda\phi\,, \tag{3.2 a}$$

$$D_0\left(\varepsilon A_e^2\psi_x + 2A_e v_{ex}\phi\right)_x - 3\varepsilon^2 A_e^2 v_e\phi - \varepsilon^3\psi A_e^3 = \tau\lambda\varepsilon^2\left(\varepsilon A_e^2\psi + 2A_e v_e\phi\right)\,. \tag{3.2 b}$$

We consider (3.2 a) and (3.2 b) on $|x| \le l$ subject to the Floquet-type boundary conditions

$$\phi(l) = z\phi(-l)\,, \qquad \phi'(l) = z\phi'(-l)\,, \qquad \psi(l) = z\psi(-l)\,, \qquad \psi'(l) = z\psi'(-l)\,, \tag{3.2 c}$$

where z is a complex parameter.

For simplicity, in this section we will set $\tau = 0$ in (3.2 b). The analysis of the possibility of Hopf bifurcations induced by taking $\tau \neq 0$ is studied in §4.

After formulating the NLEP associated with solving (3.2) for arbitrary z, we then must determine z so that we have the required NLEP problem for a K-hot-spot pattern on $[-l,(2K-1)l]$ with periodic boundary conditions. This is done by translating ϕ and ψ from the interval $[-l,l]$ to the extended interval $[-l,(2K-1)l]$ in such a way that the extended ϕ and ψ have continuous derivatives at $x = l, 3l, \ldots, (2K-3)l$. It follows that $\phi\,[(2K-1)l] = z^K\phi(-l)$, and hence to obtain periodic boundary conditions on an interval of length $2Kl$ we require that $z^K = 1$, so that

$$z_j = e^{2\pi i j/K}\,, \qquad j = 0,\ldots,K-1\,. \tag{3.3}$$

By using these values of z_j in the NLEP problem associated with (3.2), we obtain the stability threshold of a K-hot-spot solution on a domain of length $2Kl$ subject to periodic boundary conditions. The last step in the analysis is then to extract the stability thresholds for the corresponding Neumann problem from the thresholds for the periodic problem, and to choose l appropriately so that the Neumann problem is posed on $[-1,1]$. This is done below. This Floquet-based approach to determine the NLEP problem of a K-hot-spot steady-state solution for the Neumann problem has been used previously for reaction-diffusion systems exhibiting mesa patterns [**22**], for the Gierer-Meinhardt model [**34**], and for a cross-diffusion system [**19**].

We now implement the details of this calculation. The asymptotic analysis for $\varepsilon \to 0$ of (3.2) proceeds as follows. In the inner region with $y = \varepsilon^{-1}x$, we use $A_e = \mathcal{O}(\varepsilon^{-1})$ and $v_{ex} \ll 1$, to obtain from (3.2 b) that to leading order $\left[w^2\psi_y\right]_y = 0$ in the inner region, where w is the homoclinic satisfying (2.10). To prevent exponential growth for ψ as $|y| \to \infty$, we must take $\psi = \psi_0$ where ψ_0 is a constant to be determined. Then, for (3.2 a) we look for a localized inner eigenfunction in the form

$$\phi \sim \Phi(y)\,, \qquad y = \varepsilon^{-1}x\,.$$

Upon using the leading-order approximation $A_e \sim \varepsilon^{-1}v_0^{-1/2}w$ in (3.2 a), we obtain to leading order that $\Phi(y)$ satisfies

$$L_0\Phi + \frac{1}{v_0^{3/2}}w^3\psi_0 = \lambda\Phi\,, \qquad -\infty < y < \infty\,; \qquad L_0\Phi \equiv \Phi'' - \Phi + 3w^2\Phi\,, \tag{3.4}$$

with $\Phi \to 0$ as $|y| \to \infty$. Here v_0 is given in (2.16).

In the outer region, away from the hot-spot centered at $x = 0$, we have $A_e \sim \alpha$ and $v = \mathcal{O}(1)$, so that (3.2 *a*) yields

$$\phi = \frac{\varepsilon^3 \alpha^3}{\lambda + 1} \psi \,. \tag{3.5}$$

Then, from (3.2 *b*), together with $A_e \sim \alpha$, we obtain the outer approximation $D_0 \left[\varepsilon \alpha^2 \psi_x + \mathcal{O}(\varepsilon^3) \right]_x = \mathcal{O}(\varepsilon^3)$, which yields the leading-order outer problem

$$\psi_{xx} = 0 \,, \qquad 0 < |x| \le l \,, \tag{3.6}$$

subject to the Floquet-type boundary conditions (3.2 *c*). The matching condition for the inner and outer representations of ψ is that $\lim_{x \to 0} \psi(x) = \psi_0$, where ψ_0 is the unknown constant required in the spectral problem (3.4). However, the problem for ψ is not yet complete, as it must be supplemented by appropriate jump conditions for ψ_x across $x = 0$.

We now proceed to derive this jump condition. We first define an intermediate scale η satisfying $\varepsilon \ll \eta \ll 1$, and we integrate (3.2 *b*) over $|x| \le \eta$ to get

$$D_0 \left(\varepsilon A_e^2 \psi_x + 2 A_e v_{ex} \phi \right) |_{-\eta}^{\eta} = \int_{-\eta}^{\eta} \left(3\varepsilon^2 A_e^2 v_e \phi + \varepsilon^3 \psi A_e^3 \right) \, dx \,. \tag{3.7}$$

We use the limiting behavior as $x \to 0^{\pm}$ of the outer expansion to calculate the terms on the left hand-side of (3.7). From $A_e \sim \alpha$, (2.14) to calculate $v_{ex}(0^{\pm})$, and (3.5) to calculate $\phi(0^{\pm})$, we obtain that

$$D_0 \left(\varepsilon A_e^2 \psi_x \right) |_{-\eta}^{\eta} \sim D_0 \varepsilon \alpha^2 \left(\psi_x(0^+) - \psi_x(0^-) \right) = \varepsilon D_0 \alpha^2 \left[\psi_x \right]_0 \,, \tag{3.8 a}$$

$$D_0 \left(2 A_e v_{ex} \phi \right) |_{-\eta}^{\eta} \sim 2 D_0 \alpha \left[\phi(0^+) v_{ex}(0^+) - \phi(0^-) v_{ex}(0^-) \right] = 4 D_0 \alpha \phi(0^+) v_{ex}(0^+) \sim \frac{4\varepsilon^3 \alpha^2}{\lambda + 1} \psi(0) (\gamma - \alpha) l \,. \tag{3.8 b}$$

Here we have defined $[\psi_x]_0 \equiv \psi_x(0^+) - \psi_x(0^-)$.

Next, since $\eta \gg \mathcal{O}(\varepsilon)$, we can estimate the integrals on the right-hand side of (3.7) by their contributions from the inner approximation $A_e \sim \varepsilon^{-1} v_0^{-1/2} w(y)$, $\psi \sim \psi_0$, $\phi \sim \Phi(y)$, and $v_e \sim v_0$. In this way, we calculate

$$\int_{-\eta}^{\eta} \left(3\varepsilon^2 A_e^2 v_e \phi + \varepsilon^3 \psi A_e^3 \right) \, dx \sim 3\varepsilon \int_{-\infty}^{\infty} w^2 \Phi \, dy + \frac{\varepsilon \psi_0}{v_0^{3/2}} \int_{-\infty}^{\infty} w^3 \, dy \,. \tag{3.9}$$

Upon substituting (3.8) and (3.9) into (3.7), we obtain the following jump condition for ψ_x across $x = 0$:

$$D_0 \alpha^2 \left[\psi_x \right]_0 = \psi_0 \left(v_0^{-3/2} \int_{-\infty}^{\infty} w^3 \, dy - \frac{4\varepsilon^2 \alpha^2}{\lambda + 1} (\gamma - \alpha) l \right) + 3 \int_{-\infty}^{\infty} w^2 \Phi \, dy \,. \tag{3.10}$$

For the range $\lambda > -1$, we can neglect the negligible $\mathcal{O}(\varepsilon^2)$ term in the jump condition (3.10). In this way, the problem for the outer eigenfunction $\psi(x)$ is to solve

$$\psi_{xx} = 0 \,, \qquad 0 < |x| \le l \,; \qquad \psi(l) = z \psi(-l) \,, \quad \psi'(l) = z \psi'(-l) \,, \tag{3.11 a}$$

subject to the continuity condition $\psi(0^+) = \psi(0^-) = \psi_0$ and the following jump condition across $x = 0$:

$$a_0 \left[\psi_x \right]_0 + a_1 \psi(0) = a_2 \,; \qquad a_0 \equiv D_0 \alpha^2 \,, \qquad a_1 = -v_0^{-3/2} \int_{-\infty}^{\infty} w^3 \, dy \,, \qquad a_2 = 3 \int_{-\infty}^{\infty} w^2 \Phi \, dy \,. \tag{3.11 b}$$

Upon calculating $\psi(0) = \psi_0$ from this problem, the NLEP is then obtained from (3.4).

Upon solving (3.11) for $\psi(x)$, and evaluating the result at $x = 0$ we get

$$v_0^{-3/2} \psi_0 = -3 \left(\frac{\int_{-\infty}^{\infty} w^2 \Phi \, dy}{\int_{-\infty}^{\infty} w^3 \, dy} \right) \left[1 - \left(\frac{D_0 \alpha^2 v_0^{3/2}}{2l \int_{-\infty}^{\infty} w^3 \, dy} \right) \frac{(z-1)^2}{z} \right]^{-1} \,. \tag{3.12}$$

Next, we use (2.16) for v_0 and $\int_{-\infty}^{\infty} w^3\,dy = \sqrt{2}\pi$ to simplify $v_0^{-3/2}\psi_0$. In addition, we use (3.3) to calculate

$$\frac{(z-1)^2}{z} = -2 + 2\mathrm{Re}(z) = -2\left[1-\cos\left(2\pi j/K\right)\right], \quad j = 0,\ldots,K-1\,. \tag{3.13}$$

Upon substituting these results into (3.4), we obtain the following NLEP for a K-hot-spot steady-state on a domain of length $2Kl$ subject to periodic boundary conditions:

$$L_0\Phi - \chi_j w^3 \frac{\int_{-\infty}^{\infty} w^2\Phi\,dy}{\int_{-\infty}^{\infty} w^3\,dy} = \lambda\Phi\,, \qquad -\infty < y < \infty\,; \qquad \Phi\to 0\,, \quad |y|\to\infty\,, \tag{3.14 a}$$

$$\chi_j \equiv 3\left[1 + \frac{D_0\alpha^2\pi^2}{4l^4(\gamma-\alpha)^3}\left(1-\cos\left(2\pi j/K\right)\right)\right]^{-1}, \quad j = 0,\ldots,K-1\,. \tag{3.14 b}$$

The final step in the analysis is extract the NLEP for the Neumann problem from the NLEP (3.14) for the periodic problem. More specifically, the stability thresholds for a K-hot-spot pattern with Neumann boundary conditions can be obtained from the corresponding thresholds for a $2K$-hot-spot pattern with periodic boundary conditions on a domain of twice the length. To see this, suppose that ϕ is a Neumann eigenfunction on the interval $[0,a]$. Extend it by an even reflection about the origin to the interval $[-a,a]$. Such an extension then satisfies periodic boundary conditions on $[-a,a]$. Alternatively, if $\phi(x)$ is an eigenfunction with periodic boundary conditions at the edge of the interval $[-a,a]$, then define $\hat{\phi}(x) = \phi(x) + \phi(-x)$. Then, $\hat{\phi}$ is a eigenfunction for the Neumann boundary problem on $[0,a]$.

Therefore, to obtain the NLEP problem governing the stability of an steady-state K-hot-spot pattern on an interval of length S subject to Neumann boundary conditions, we simply replace $\cos(2\pi j/K)$ with $\cos(\pi j/K)$ in (3.14) and then set $l = S/(2K)$ in the NLEP of (3.14). In this way, we obtain the following main result:

Principal Result 3.1: *Consider a K-hot-spot solution to (2.5) on an interval of length S subject to Neumann boundary conditions. For $\varepsilon\to 0$, and $\tau = \mathcal{O}(1)$, the stability of this solution with respect to the "large" eigenvalues $\lambda = O(1)$ of the linearization is determined by the spectrum of the NLEP*

$$L_0\Phi - \chi_j w^3 \frac{\int_{-\infty}^{\infty} w^2\Phi\,dy}{\int_{-\infty}^{\infty} w^3\,dy} = \lambda\Phi\,, \qquad -\infty < y < \infty\,; \qquad \Phi\to 0\,, \quad |y|\to\infty\,, \tag{3.15 a}$$

$$\chi_j = 3\left[1 + \frac{D_0\alpha^2\pi^2K^4}{4(\gamma-\alpha)^3}\left(\frac{2}{S}\right)^4\left(1-\cos\left(\pi j/K\right)\right)\right]^{-1}, \quad j = 0,\ldots,K-1\,, \tag{3.15 b}$$

where $w(y)$ is the homoclinic solution satisfying $w'' - w + w^3 = 0$.

The stability threshold for D_0 is characterized by the largest possible value of D_0 for which the point spectrum of (3.15) satisfies $\mathrm{Re}(\lambda) < 0$ for each $j = 0,\ldots,K-1$. In contrast to the typical NLEP problem associated with spike patterns in the Gierer-Meinhardt, Gray-Scott, and Schnakeneburg reaction-diffusion models studied in [**3**], [**4**], [**5**], [**10**], [**15**], [**35**], [**36**], and [**43**], the point spectrum for the non-self-adjoint problem (3.15) is real, and can be determined analytically. This fact, as we now show, relies critically on the identity $L_0w^2 = 3w^2$ from (2.12).

Lemma 3.2: *Consider the NLEP problem*

$$L_0\Phi - cw^3\int_{-\infty}^{\infty} w^2\Phi\,dy = \lambda\Phi\,, \qquad -\infty < y < \infty\,; \qquad \Phi\to 0\,, \quad |y|\to\infty\,, \tag{3.16}$$

for an arbitrary constant c corresponding to eigenfunctions for which $\int_{-\infty}^{\infty} w^2\Phi\,dy \neq 0$. Consider the range $Re(\lambda) >$

-1. *Then, on this range there is only one element in the point spectrum, and it is given explicitly by*

$$\lambda = 3 - c\int_{-\infty}^{\infty} w^5\,dy\,. \tag{3.17}$$

To prove this we consider only the region $\mathrm{Re}(\lambda) > -1$, where we can guarantee that $|\Phi| \to 0$ exponentially as $|y| \to \infty$. The continuous spectrum for (3.16) is $\lambda < -1$, with λ real. To establish (3.17) we use Green's identity on w^2 and Φ, which is written as $\int_{-\infty}^{\infty}\left(w^2 L_0\Phi - \Phi L_0 w^2\right)\,dy = 0$. Since $L_0\Phi = cw^3\int_{-\infty}^{\infty} w^2\Phi\,dy + \lambda\Phi$ and $L_0 w^2 = 3w^2$, this identity reduces to

$$\int_{-\infty}^{\infty} w^2\Phi\,dy\left(\lambda - 3 + c\int_{-\infty}^{\infty} w^5\,dy\right) = 0\,,$$

from which the result (3.17) follows. We remark that for the corresponding local eigenvalue problem $L_0\Phi = \nu\Phi$, it was proved in Proposition 5.6 of [**3**] that the point spectrum consists only of $\nu_0 = 3$ and the translation mode $\nu_1 = 0$ (with odd eigenfunction), and that there are no other point spectra in $-1 < \nu < 0$. When $c = 0$, we observe that (3.17) agrees with ν_0. As a further remark, the result (3.17), when extrapolated into the region $\lambda < -1$, suggests that there is a critical value of c for which the discrete eigenvalue bifurcates out of the continuous spectrum into the region $\lambda > -1$ on the real axis.

By applying Lemma 3.2 to the NLEP (3.15) we conclude that $\mathrm{Re}(\lambda) < 0$ if and only if

$$\chi_j > 3\left(\frac{\int_{-\infty}^{\infty} w^3\,dy}{\int_{-\infty}^{\infty} w^5\,dy}\right) = 2\,, \qquad j = 0,\ldots,K-1\,. \tag{3.18}$$

In obtaining the last equality in (3.18) we calculated the integrals using $w = \sqrt{2}\,\mathrm{sech}\,y$. Since $\chi_0 = 3 > \chi_1 > \chi_2 > \ldots > \chi_{K-1}$, a one-hot-spot solution is stable for all D_0, while the instability threshold for a multi hot-spot pattern is set by χ_{K-1}. In this way, we obtain the following main stability result.

Principal Result 3.2: *Consider a K-hot-spot solution to (2.5) on an interval of length S with $K > 1$ subject to Neumann boundary conditions. For $\tau = 0$, and in the limit $\varepsilon \to 0$, this solution is stable on an $\mathcal{O}(1)$ time-scale provided that $D_0 < D_{0K}^L$, where*

$$D_{0\mathrm{K}}^L \equiv \frac{2(\gamma-\alpha)^3\,(S/2)^4}{K^4\alpha^2\pi^2\,[1+\cos(\pi/K)]}\,. \tag{3.19}$$

In terms of the original diffusivity D, given by $D = \varepsilon^{-2}D_0$, the stability threshold is $D_K^L = \varepsilon^{-2}D_{0K}^L$ when $K > 1$. Alternatively, a one-hot-spot solution is stable for all $D_0 > 0$, provided that D_0 is independent of ε.

Although we have not calculated the stability threshold for the small eigenvalues for which $\lambda \to 0$ as $\varepsilon \to 0$ in the spectrum of the linearization (3.2), we conjecture that this stability threshold is the same critical value $D_{0\mathrm{K}}^S$ of D_0, given in (2.22), for which an asymmetric K-hot-spot steady-state branch bifurcates off of the symmetric K-hot-spot branch. This simple approach to calculate the small eigenvalue stability threshold, which avoids the lengthy matrix manipulations of [**10**], has been validated for the Gierer-Meinhardt, Gray-Scott, and Schnakenburg reaction-diffusion models in [**37**], [**36**], and [**18**]. Since $D_{0\mathrm{K}}^S < D_{0\mathrm{K}}^L$ for $K \geq 2$, we conclude that a symmetric K-hot-spot steady-state solution is stable with respect to both the large and the small eigenvalues only when $D < D_{0\mathrm{K}}^S$.

We make two remarks. Firstly, for the case of a single hot-spot where $K = 1$ we expect that the stability threshold for D_0 will be exponentially large in $1/\varepsilon$, and similar to that derived in [**14**] for the Gierer-Meinhardt model in the near-shadow limit. Secondly, we remark that the possibility of stabilizing multiple hot-spots for (2.1) is in direct contrast to the result obtained in the analysis of [**32**] of spike solutions for a Keller-Segel-type chemotaxis model with

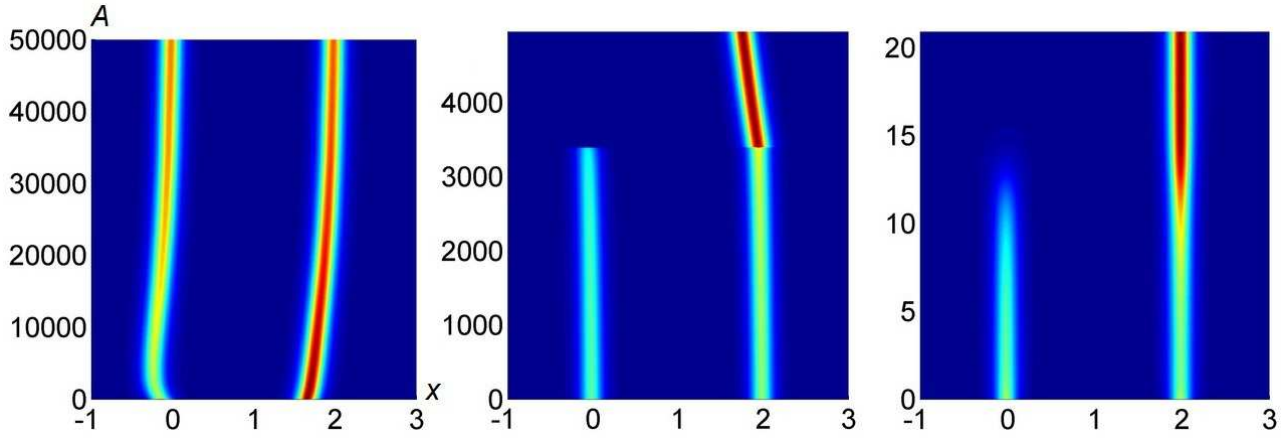

Figure 3. Instabilities of a two-hot-spot steady-state solution induced by increasing D. Left: two hot-spots are stable with $D = 15$. Middle: two hot-spots exhibit a slow-time instability when $D = 30$. Right: there is a fast-time instability when $D = 50$. The parameter values are fixed at $\varepsilon = 0.07$ $\alpha = 1$, and $\gamma = 2$, on the interval $x \in [-1, 3]$. The initial condition for the full numerical solution of (2.3) consists of two hot-spots that are perturbed slightly from the steady-state locations.

a logarithmic sensitivity function for the drift term. For this chemotaxis problem of [**32**], only a one-spike solution can be stable.

3.1 Numerical Results

We now compare our stability predictions with results from full numerical solutions of (2.3). As derived above, under Neumann boundary conditions the thresholds on D for the stability of a symmetric K-hot-spot pattern on a domain of length $2KL$ are

$$D_{\rm K}^S \sim \frac{L^4}{\varepsilon^2}\frac{(\gamma-\alpha)^3}{\alpha^2\pi^2}\,, \qquad D_{0K}^L = D_{0K}^S\left(\frac{2}{1+\cos(\pi/K)}\right). \tag{3.20}$$

To numerically validate these thresholds, we choose $\varepsilon = 0.07$, $\alpha = 1$, $\gamma = 2$, $L = 1$ and $K = 2$, so that we have an interval of length $S = 4$. For these parameters, our predicted stability thresholds are $D_{\rm K}^S \approx 20.67$ and $D_{\rm K}^L \approx 41.33$, and our initial condition is a two-hot-spot solution with hot-spot locations slightly perturbed from their steady-state values. For our full numerical solutions of (2.3) we choose either $D = 15$, $D = 30$, or $D = 50$. Our stability theory predicts the following; the two hot-spots are stable when $D = 15$; the two hot-spots are unstable with respect to only the small eigenvalues when $D = 30$; the two hot-spots are unstable with respect to both the small and large eigenvalues when $D = 50$. The full numerical results shown in Fig. 3 confirm this prediction from the asymptotic theory.

4 Hopf Bifurcation of K-Hot-Spot Steady-State Solutions

In this section we study the spectrum of (3.2) for $\tau > 0$. This is done by first deriving an NLEP similar to (3.15). Since the analysis leading to the new NLEP is very similar to that in §3, we will only outline it here briefly.

For $\tau \ll \mathcal{O}(\varepsilon^2)$, we get $\psi \approx \psi_0$ in the inner region $x = \mathcal{O}(\varepsilon)$, and hence (3.4) for the inner approximation $\Phi(y)$ for ϕ remains valid. For $\tau \ll \mathcal{O}(\varepsilon^2)$, we get to leading-order that $\psi_{xx} = 0$ in the outer region $0 < |x| \le l$ and so (3.6)

still holds. However, for $\tau \neq 0$, the jump conditions (3.7)–(3.9) must be modified. In place of (3.7), we get

$$D_0\left(\varepsilon A_e^2\psi_x + 2A_e v_{ex}\phi\right)|_{-\eta}^{\eta} = \int_{-\eta}^{\eta}\left(3\varepsilon^2 A_e^2 v_e\phi + \varepsilon^3\psi A_e^3\right)\,dx + \varepsilon^2\tau\lambda\int_{-\eta}^{\eta}\left(\varepsilon A_e^2\psi + 2A_e v_e\phi\right)\,dx\,. \tag{4.1}$$

The left hand-side of (4.1) was estimated in (3.8), while the first two terms on the right-hand side of (4.1) were estimated in (3.9). We then use $A_e \sim \varepsilon^{-1}v_0^{-1/2}w(y)$, $\psi \sim \psi_0$, $\phi \sim \Phi(y)$, and $v_e \sim v_0$, to estimate the last term on the right hand-side of (4.1) as

$$\varepsilon^2\tau\lambda\int_{-\eta}^{\eta}\left(\varepsilon A_e^2\psi + 2A_e v_e\phi\right)\,dx \sim \varepsilon^2\tau\lambda\left[\frac{\psi_0}{v_0}\int_{-\infty}^{\infty}w^2\,dy + 2\sqrt{v_0}\int_{-\infty}^{\infty}w\Phi\,dy\right]\,. \tag{4.2}$$

Upon substituting (3.8), (3.9), and (4.2), into (4.1), we obtain that

$$D_0\varepsilon\alpha^2\left[\psi_x\right]_0 + \mathcal{O}(\varepsilon^3) = \varepsilon\left[3\int_{-\infty}^{\infty}w^2\Phi\,dy + \frac{\psi_0}{V_0^{3/2}}\int_{-\infty}^{\infty}w^3\,dy\right] + \varepsilon^2\tau\lambda\left[\frac{\psi_0}{v_0}\int_{-\infty}^{\infty}w^2\,dy + 2\sqrt{v_0}\int_{-\infty}^{\infty}w\Phi\,dy\right]\,, \tag{4.3}$$

which suggests the distinguished limit $\tau = \mathcal{O}(\varepsilon^{-1})$. Upon defining $\tau_0 = \mathcal{O}(1)$ by

$$\tau = \varepsilon^{-1}\tau_0\,, \tag{4.4}$$

(4.3) yields the jump condition (3.11 *b*) for ψ across $x = 0$, where a_0, a_1, and a_2 in (3.11 *b*) are to be replaced by

$$a_0 = D\alpha^2\,, \qquad a_1 = -v_0^{-3/2}\int_{-\infty}^{\infty}w^3\,dy - \frac{\tau_0\lambda}{v_0}\int_{-\infty}^{\infty}w^2\,dy\,, \qquad a_2 = 3\int_{-\infty}^{\infty}w^2\Phi\,dy + 2\sqrt{v_0}\tau_0\lambda\int_{-\infty}^{\infty}w\Phi\,dy\,. \tag{4.5}$$

With this modification of the coefficients in (3.11 *b*), the outer problem for ψ is still (3.11).

This problem is readily solved for $\psi(x)$, and we obtain that $\psi_0 = \psi(0)$ is given by

$$v_0^{-3/2}\psi_0 = -\left[3\left(\frac{\int_{-\infty}^{\infty}w^2\Phi\,dy}{\int_{-\infty}^{\infty}w^3\,dy}\right) + 2\tau_0\lambda\sqrt{v_0}\left(\frac{\int_{-\infty}^{\infty}w\Phi\,dy}{\int_{-\infty}^{\infty}w^3\,dy}\right)\right]\left[1 - \frac{D_0\alpha^2\pi^2(z-1)^2}{8l^4(\gamma-\alpha)^3 z} + \frac{2\tau_0\lambda}{l(\gamma-\alpha)}\right]^{-1}\,. \tag{4.6}$$

Finally, upon substituting (2.16) and (3.13) into (4.6), the NLEP problem for the Floquet problem on $[-l, l]$ follows from (3.4). As shown in §3, this problem allows us to readily determine the corresponding NLEP for the Neumann boundary condition problem on an interval of length S. The result is summarized as follows:

Principal Result 4.1: *Let $\tau = \mathcal{O}(\varepsilon^{-1})$ as $\varepsilon \to 0$ and consider a steady-state k-hot-spot solution on an interval of length S with Neumann boundary conditions. Define $\tau_c = \mathcal{O}(1)$ by $\tau = \varepsilon^{-1}S(\gamma-\alpha)\tau_c/(4K)$. Then, the stability of a symmetric K-hot-spot steady-state solution is determined by the NLEP*

$$L_0\Phi - 3\chi_j w^3\left(\frac{\int_{-\infty}^{\infty}w^2\Phi\,dy}{\int_{-\infty}^{\infty}w^3\,dy}\right) - \frac{\chi_{1j}}{2}w^3\int_{-\infty}^{\infty}w\Phi\,dy = \lambda\Phi\,, \qquad -\infty < y < \infty\,, \tag{4.7 a}$$

with $\Phi \to 0$ as $|y| \to \infty$. Here, we have defined χ_j, χ_{1j}, and β_j by

$$\chi_j \equiv \frac{1}{[\beta_j + \tau_c\lambda]}\,, \qquad \chi_{1j} \equiv (\tau_c\lambda)\chi_j\,, \qquad \beta_j \equiv 1 + \frac{D_0\alpha^2\pi^2K^4}{4(\gamma-\alpha)^3}\left(\frac{2}{S}\right)^4\left(1-\cos\left(\pi j/K\right)\right)\,, \quad j = 0,\ldots,K-1\,. \tag{4.7 b}$$

This NLEP, with two separate nonlocal terms, is significantly different in form from the NLEP's derived for the Gierer-Meinhardt and Gray-Scott models studied in [**3**], [**4**], [**5**], [**35**], and [**15**].

Principal Result 4.2: *There is no value of $\tau_c > 0$ for which the NLEP of (4.7) has a Hopf bifurcation.*

We note that there is a key step in the derivation of Principal Result 4.2 which relies on a numerical computation, see below. A completely computer-free derivation of this result is still an open problem.

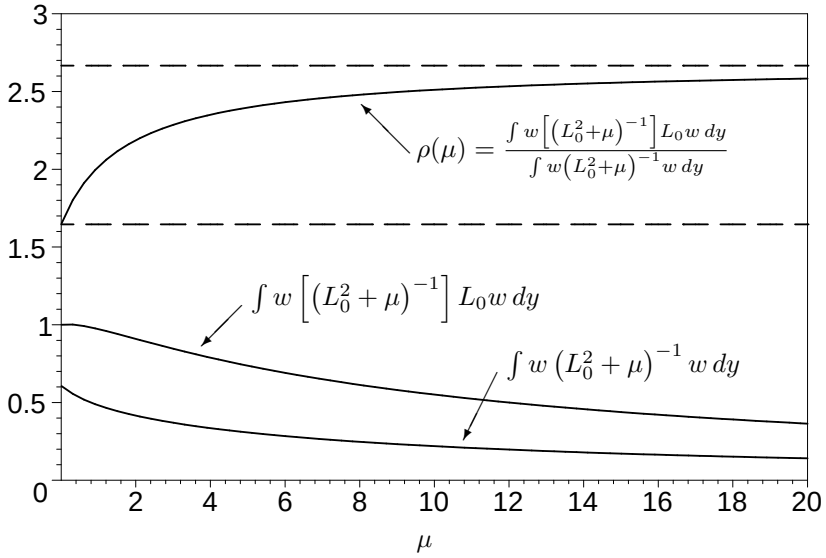

Figure 4. A plot of the numerical result for $\rho(\mu)$, as obtained from (4.12). Note that $\rho(\mu)$ is monotone increasing.

Derivation of Principal Result 4.2: We use the notation $\int h\, dy \equiv \int_\infty^\infty h\, dy$. Upon using Green's identity $\int w^2 L\Phi\, dy = \int \Phi L w^2\, dy$ and $L_0 w^2 = 3w^2$, together with (4.7 a), we obtain

$$\left(3 - 3\chi_j \frac{\int w^5\, dy}{\int w^3\, dy}\right) \int w^2\Phi\, dy - \frac{\chi_{1j}}{2}\left(\int w^5\, dy\right)\left(\int w\Phi\, dy\right) = \lambda \int w^2\Phi\, dy\,.$$

Upon solving for $\int w^2\Phi\, dy$ in terms of $\int w\Phi\, dy$, and then substituting into (4.7 a), we get

$$L_0\Phi - f(\lambda) w^3 \int w\Phi\, dy = \lambda\Phi\,, \qquad f(\lambda) = \left[\frac{2}{\chi_{1j}} - \frac{6\chi_j}{\chi_{1j}(3-\lambda)}\left(\frac{\int w^5\, dy}{\int w^3\, dy}\right)\right]^{-1}. \tag{4.8 a}$$

We then simplify $f(\lambda)$ by using (4.7 b), together with $\int w^5 = (3/2)\int w^3$, to obtain

$$\frac{1}{f(\lambda)} = \frac{2\beta_j}{\tau_c\lambda} + 2 - \frac{9}{\tau_c\lambda(3-\lambda)}\,. \tag{4.8 b}$$

Next, we observe that the eigenvalues λ of the NLEP problem (4.8) are the roots of the transcendental equation

$$\frac{1}{f(\lambda)} = \int w\,(L_0 - \lambda)^{-1} w^3\, dy\,. \tag{4.9}$$

Upon recalling that $L_0 w = 2w^3$, we calculate

$$\int w\,(L_0-\lambda)^{-1} w^3\, dy = \frac{1}{2}\int w\,(L_0-\lambda)^{-1}\left[(L_0-\lambda)w + \lambda w\right] dy = \frac{1}{2}\int w^2\, dy + \frac{\lambda}{2}\int w\,(L_0-\lambda)^{-1} w\, dy\,.$$

Substituting this result together with (4.8 b) and $\int w^2 = 4$ into (4.9), we obtain that λ is a root of

$$\frac{\lambda}{2}\int w\,(L_0-\lambda)^{-1} w\, dy = \frac{2\beta_j}{\tau_c\lambda} - \frac{9}{\tau_c\lambda(3-\lambda)}\,. \tag{4.10}$$

To determine whether a Hopf bifurcation is possible we set $\lambda = i\lambda_I$ in (4.10) and replace $(L_0-\lambda)^{-1}$ by $(L_0-\lambda)^{-1} = \left(L_0^2+\lambda_I^2\right)^{-1}(L_0 + i\lambda_I)$. Then, upon comparing the real and imaginary parts in the resulting expression, we obtain that $\mu \equiv \lambda_I^2$ and any Hopf bifurcation threshold τ_c must be the roots of the coupled system

$$\int w\left[\left(L_0^2+\mu\right)^{-1}\right] L_0 w\, dy = -\frac{4\beta_j}{\tau_c\mu} + \frac{54}{\tau_c\mu(9+\mu)}\,, \qquad \int w\left(L_0^2+\mu\right)^{-1} w\, dy = \frac{18}{\tau_c\mu(9+\mu)}\,. \tag{4.11}$$

Upon eliminating τ_c from (4.11), we obtain a transcendental equation solely for $\mu = \lambda_I^2 > 0$,

$$\rho(\mu) = 3 - 2\beta_j \; - \frac{2\beta_j}{9}\mu\,, \qquad \text{where} \qquad \rho(\mu) \equiv \frac{\int w\left[\left(L_0^2+\mu\right)^{-1}\right] L_0 w\, dy}{\int w\left(L_0^2+\mu\right)^{-1} w\, dy}\,. \tag{4.12}$$

By using the identities $L_0 w = 2w^3$ and $L_0^{-1} w = (w + yw')/2$, the limiting behavior for $\rho(\mu)$ is readily calculated as

$$\rho(\infty) = \frac{\int w L_0 w\, dy}{\int w^2\, dy} = \frac{8}{3}\,; \qquad \rho(0) = \frac{\int w L_0^{-1} w\, dy}{\int \left(L_0^{-1} w\right)^2\, dy} = \frac{36}{\pi^2+12} \approx 1.6461\,.$$

Moreover, **direct numerical computations** of $\rho(\mu)$ show that it is an increasing function of μ (see Fig. 4). On the other hand, for $\mu > 0$ we have $3 - 2\beta_j \; - \frac{2\beta_j}{9}\mu < 1$ since $\beta_j \geq 1$. It follows that (4.12) cannot have any solution with $\mu > 0$. Consequently, there is no Hopf bifurcation on the parameter regime $\tau = \mathcal{O}(\varepsilon^{-1})$. ■

Such a non-existence result for Hopf bifurcations for the crime model when $\tau = \mathcal{O}(\varepsilon^{-1})$ is qualitatively very different than for the Gierer-Meinhardt and Gray-Scott models, analyzed in [**35**] and [**15**], where Hopf bifurcations occur in wide parameter regimes.

4.1 A Hopf Bifurcation for the Shadow Limit

Principal Result 4.2 has shown that there is no Hopf bifurcation for the regime $\tau = \mathcal{O}(\varepsilon^{-1})$. However, a Hopf bifurcation can and does appear when $\tau = \mathcal{O}(\varepsilon^{-2})$. As will be shown below, in such a regime the amplitude of the hot-spot becomes oscillatory with an asymptotically large temporal period, due to an eigenvalue that is dominated, to leading-order in ε, by its pure imaginary part. To illustrate this phenomenon, in this section we analytically derive the condition for a Hopf bifurcation of a single boundary spot on a domain of length one. To further simplify our computations, we will assume that D_0 in (2.5 *b*) is taken sufficiently large such that $v(x,t) = v(t)$ can be approximated by a time-dependent constant. The limit $D \to \infty$ is called the shadow-limit (cf. [**38**]). Our main result is the following:

Principal Result 4.3: *Suppose that $D_0 \gg 1$ and consider a half hot-spot of (2.5) located at the origin on the domain $[0,1]$, as constructed in Principal Result 2.1. Define τ_{0c} by*

$$\tau_{0c} = \frac{\left(24-\pi^2\right)}{36\pi^2}\frac{(\gamma-\alpha)^3}{\alpha^2} = 0.039769\frac{(\gamma-\alpha)^3}{\alpha^2}. \tag{4.13}$$

Let $\tau = \tau_0/\varepsilon^2$. Then, there is a Hopf bifurcation at $\tau_0 = \tau_{0c}$. That is, the hot spot is stable for $\tau_0 < \tau_{0c}$ and is unstable for $\tau_0 > \tau_{0c}$. Destabilization takes place via a Hopf bifurcation. More precisely, when $\tau_0 = O(1)$, the related stability problem has an eigenvalue near the origin with the following asymptotic behavior as $\varepsilon \to 0$:

$$\lambda \sim \left\{\pm\sqrt{\frac{\gamma-\alpha}{\tau_0}}\right\} i\varepsilon^{1/2} + \left\{\frac{\alpha^2\pi^2}{2(\gamma-\alpha)^2} - \frac{(\gamma-\alpha)}{\tau_0}\left(\frac{24-\pi^2}{72}\right)\right\}\varepsilon\,. \tag{4.14}$$

Numerical example. To illustrate Principal Result 4.3 we take $\gamma = 4, \alpha = 1, \varepsilon = 0.05$ and $D_0 = 1000$. Then, (4.13) yields $\tau_{0c} \approx 1.07378$. Now take $\tau_0 = 0.95$ so that (4.14) yields the eigenvalue $\lambda \approx 0.4082i - 0.00529$. We then expect the single hot-spot to be stable, although it will exhibit long transient oscillations. From the eigenvalue, we can estimate the period of the oscillation to be $P = \frac{2\pi}{0.4082} \approx 15.39$. This agrees with full numerical solutions of (4.15) as shown in Fig. 5(a).

Next, we increase τ_0 to 1.15, while keeping the other parameters the same. In this case, $\tau_0 > \tau_{0c}$ so that the hot-spot is unstable in the limit $\varepsilon \to 0$. However, $\tau_0 = 1.15$ is very close to the threshold value, and with $\varepsilon = 0.05$, we expect even longer transients with the final state still unclear at $t = 300$. This behavior is shown in Fig. 5(b).

Finally, as shown in Fig. 5(c), when we increase τ_0 to 1.35, we clearly observe oscillations of an increasing amplitude.

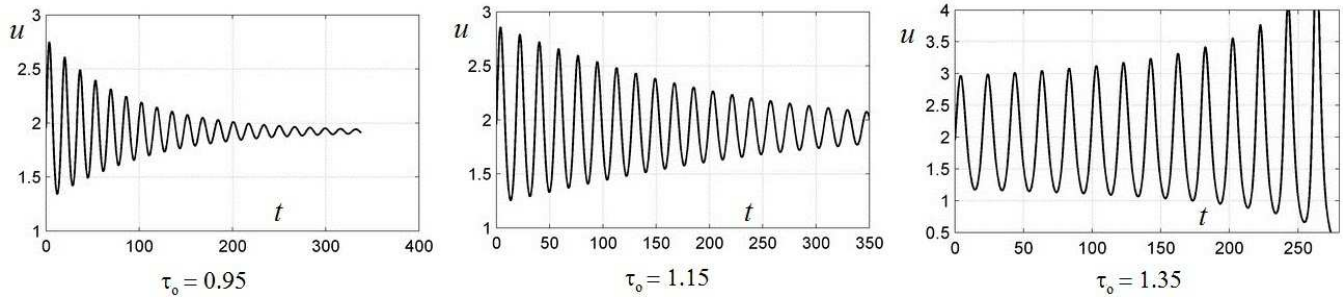

(a) (b) (c)

Figure 5. $\max u$ versus t with $\varepsilon = 0.05, \alpha = 1, \gamma = 4, \tau = \tau_0/\varepsilon^2$ with τ_0 as given in the figure. (a) $\tau_0 < \tau_c = 1.074$; damping is observed. (b) $\tau_0 > \tau_c$ but τ_0 is very close to τ_c; eventual fate of the oscillation is unclear. (c) $\tau_0 > \tau_c$; oscillations of increasing amplitude are observed.

Derivation of Principal Result 4.3: We begin by re-writing (2.5) as a shadow system. For convenience, we also rescale A as $A = u/\varepsilon$. In terms of this scaling, $u = \mathcal{O}(1)$ in the interior of the hot-spot. Expanding v in powers of $\mathcal{D}_0^{-1}$ we then obtain to leading order that $v(x,t) \sim v(x)$. We then integrate (2.5 b) and use the no-flux boundary conditions to obtain the following shadow-limit system on $x \in [0,1]$:

$$u_t = \varepsilon^2 u_{xx} - u + vu^3 + \varepsilon\alpha\,, \qquad \tau\left(v\int_0^1 u^2\,dx\right)_t = \mu - \frac{1}{\varepsilon}v\int_0^1 u^3\,dx\,; \qquad u_x(0,t) = u_x(1,t) = 0\,, \tag{4.15 a}$$

where we have defined μ by

$$\mu \equiv \gamma - \alpha\,. \tag{4.15 b}$$

The shadow problem (4.15) is the starting point of our analysis. The corresponding steady-state system is

$$0 = \varepsilon^2 u_{xx} - u + vu^3 + \varepsilon\alpha\,, \qquad \mu = \frac{1}{\varepsilon}v\int_0^1 u^3\,dx\,; \qquad u_x(0,t) = u_x(1,t) = 0\,. \tag{4.16}$$

As shown below, in order to analyze the Hopf bifurcation it is necessary to construct the steady-state solution to two orders in ε. To do so, we let $y = x/\varepsilon$ and we expand

$$u = u_0 + \varepsilon u_1 \ldots\,, \qquad v = v_0 + \varepsilon v_1 + \ldots\,. \tag{4.17}$$

By substituting this expansion into (4.16), and equating powers of ε, we obtain that $u_0 = v_0^{-1/2} w$, where $w(y)$ is the positive homoclinic solution of $w_{yy} - w + w^3 = 0$. In addition, u_1 satisfies

$$L_0 u_1 = -\alpha - w^3 v_1 v_0^{-3/2}\,, \tag{4.18}$$

where the operator L_0 is defined by $L_0 u \equiv u_{yy} - u + 3w^2 u$. This operator has several key readily derivable identities,

$$L_0(1) = -1 + 3w^2\,, \qquad L_0 w = 2w^3\,, \qquad L_0 w^2 = 3w^2\,,$$

which allows us to determine the solution u_1 to (4.18) as

$$u_1 = \alpha - \alpha w^2 - \frac{v_1}{2v_0^{3/2}}w\,. \tag{4.19}$$

Next, to determine v_0 and v_1 we must calculate the integral in (4.16) for $\varepsilon \ll 1$. This yields that

$$\mu = \frac{1}{\varepsilon}\int_0^1 vu^3\,dx \sim \int_0^{1/\varepsilon}(v_0+\varepsilon v_1)\left(u_0^3+3u_0^2u_1\varepsilon\right)\,dy \sim v_0^{-1/2}\int_0^\infty w^3\,dy + \varepsilon\int_0^\infty \left(3u_0^2u_1v_0+v_1u_0^3\right)\,dy + \mathcal{O}(\varepsilon^2)\,.$$

By equating coefficients of ε, we get that v_0 and v_1 satisfy

$$v_0^{-1/2}\int_0^\infty w^3 dy = \mu\,, \qquad \int_0^\infty 3u_1w^2\,dy + v_1v_0^{-3/2}\int_0^\infty w^3\,dy = 0\,.$$

Upon using the solution (4.19) for u_1, the unknown v_1 can be determined in terms of a quadrature as

$$v_1 = 6\alpha v_0^{3/2}\frac{\int_0^\infty\left(w^2-w^4\right)\,dy}{\int_0^\infty w^3\,dy}\,.$$

The integrals defining v_0 and v_1 are then calculated explicitly by using

$$w = \sqrt{2}\,\operatorname{sech} y\,, \qquad \int_{-\infty}^\infty w^2\,dy = 4\,, \qquad \int_{-\infty}^\infty w^3\,dy = \int_{-\infty}^\infty w\,dy = \sqrt{2}\pi\,, \qquad \int_{-\infty}^\infty w^4\,dy = \frac{16}{3}\,,$$

which yields the explicit formulae

$$v_0 = \frac{\pi^2}{2}\mu^{-2}\,, \qquad v_1 = -2\alpha\pi^2\mu^{-3}\,. \tag{4.20}$$

Next, we study the stability of this solution. For convenience, we extend the problem to the interval $[-1,1]$ by even reflection. We linearize (4.15) around the steady-state solution to obtain the eigenvalue problem

$$\lambda\phi = \varepsilon^2\phi'' - \phi + 3u^2v\phi + u^3\psi\,; \qquad \tau\lambda\int_{-1/\varepsilon}^{1/\varepsilon}\left(2\phi uv+u^2\psi\right)\,dy = \frac{-1}{\varepsilon}\int_{-1/\varepsilon}^{1/\varepsilon}\left(3u^2v\phi+u^3\psi\right)\,dy\,,$$

where the constant ψ denotes the perturbation in v. Upon solving for ψ we obtain

$$\varepsilon^2\phi'' - \phi + 3u^2v\phi + u^3\psi = \lambda\phi\,; \qquad \psi = -\frac{\tau\lambda\varepsilon\int_{-1/\varepsilon}^{1/\varepsilon}2\phi uv\,dy + \int_{-1/\varepsilon}^{1/\varepsilon}3u^2v\phi\,dy}{\tau\lambda\varepsilon\int_{-1/\varepsilon}^{1/\varepsilon}u^2\,dy + \int_{-1/\varepsilon}^{1/\varepsilon}u^3\,dy}\,. \tag{4.21}$$

To motivate the analysis below, we first suppose that $\tau\lambda\varepsilon \gg 1$. Then, by using $u \sim w/\sqrt{v_0}$ and $v \sim v_0$, (4.21) reduces to leading order to the NLEP

$$L_0\phi - 2w^3\frac{\int\phi w}{\int w^2} = \lambda\phi\,.$$

Here and below, $\int f$ denotes $\int_{-\infty}^\infty f dy$. This problem has a zero eigenvalue corresponding to the eigenfunction $\phi = w$. All other discrete eigenvalues satisfy $\operatorname{Re}(\lambda) < 0$ (cf. [**46**]). Therefore, the critical eigenvalue will be a perturbation of the zero eigenvalue.

A posteriori computations shows that the correct anzatz is in fact

$$\lambda = \varepsilon^{1/2}\lambda_0 + \varepsilon\lambda_1 + \ldots\,; \qquad \tau = \tau_0\varepsilon^{-2}\,.$$

The analysis below shows that λ_0 is purely imaginary, and hence determines the frequency of the oscillation, but not its stability. Therefore, a two-term expansion in λ must be obtained in order to determine the stability of the oscillations. As such, we must expand all quantities in the shadow problem up to $\mathcal{O}(\varepsilon)$. The delicate part in the calculation is to note that

$$\int_{-1/\varepsilon}^{1/\varepsilon}u^2 = \int u_0^2 + \varepsilon\int 2u_0u_1 + \varepsilon^2\int_{-1/\varepsilon}^{1/\varepsilon}u_1^2\,,$$

where the last integral is in fact $\mathcal{O}(\varepsilon)$ as a result of

$$\varepsilon^2\int_{-1/\varepsilon}^{1/\varepsilon}u_1^2 = \varepsilon^2\int_{-1/\varepsilon}^{1/\varepsilon}(\alpha+\ldots)^2 = 2\alpha^2\varepsilon + \ldots$$

Thus, this term "jumps" an order and is comparable in magnitude to $\varepsilon \int 2u_0u_1$. The remaining part of the analysis is more straightforward. We let $\tau = \tau_0\varepsilon^{-2}$ and expand ψ in (4.21) as

$$\psi = -\frac{\tau\lambda\varepsilon \int 2\phi uv + \int 3u^2v\phi}{\tau\lambda\varepsilon \int u^2 + \int u^3} = \psi_0 + \varepsilon^{1/2}\psi_{1/2} + \varepsilon\psi_1\,,$$

so that the eigenvalue problem for ϕ from (4.21) becomes

$$\begin{aligned}(\varepsilon^{1/2}\lambda_0 + \varepsilon\lambda_1)\phi &= L_0\phi + (3u_0^2v_1 + 6u_0u_1v_0)\phi\varepsilon + u_0^3\left(\psi_0 + \varepsilon^{1/2}\psi_{1/2} + \varepsilon\psi_1\right) + 3u_0^2u_1\psi_0\varepsilon \\ &= L_1\phi + \varepsilon^{1/2}L_2\phi + \varepsilon L_3\phi\,. \end{aligned} \tag{4.22}$$

After tedious but straightforward computations, the three operators in (4.22) are given by

$$L_1\phi \equiv L_0\phi - 2\frac{\int w\phi}{\int w^2}w^3\,; \tag{4.23 a}$$

$$L_2\phi \equiv \psi_{1/2}u_0^3 = \left(c_0\int w\phi + c_1\int w^2\phi\right)w^3\,; \tag{4.23 b}$$

$$\begin{aligned} L_3\phi &\equiv (3u_0^2v_1 + 6u_0u_1v_0)\phi + 3u_0^2u_1\psi_0 + u_0^3\psi_1 \\ &= \left(c_2w + c_3w^2 + c_4w^3\right)\phi + \left(c_5w^2 + c_6w^3 + c_7w^4\right)\int w\phi + c_8w^3\int\phi + c_9w^3\int w^2\phi\,, \end{aligned} \tag{4.23 c}$$

in terms of the coefficients $c_0, \ldots, c_9$ defined by

$$\begin{aligned} &c_0 = \frac{\mu}{4\tau_0\lambda_0}\,; \qquad c_1 = -\frac{3\mu\sqrt{2}}{4\pi\tau_0\lambda_0}\,; \qquad c_2 = \frac{3\pi\alpha\sqrt{2}}{\mu}\,; \qquad c_3 = 0\,; \qquad c_4 = -c_2\,; \qquad c_5 = -\frac{3\sqrt{2}\pi\alpha}{4\mu} \\ &c_6 = -\frac{\mu\lambda_1}{4\tau_0\lambda_0^2} - \frac{\mu^2}{8\tau_0^2\lambda_0^2} + \frac{\pi^2\alpha^2}{8\mu^2}\,; \qquad c_7 = -c_5\,; \qquad c_8 = -\frac{\pi\sqrt{2}\alpha}{4\mu}\,; \qquad c_9 = \frac{\sqrt{2}\pi\alpha}{4\mu} + \frac{\sqrt{2}3\mu\lambda_1}{4\pi\tau_0\lambda_0^2} + \frac{\sqrt{2}3\mu^2}{8\pi\tau_0^2\lambda_0^2}\,. \end{aligned} \tag{4.24}$$

Finally, we expand ϕ in (4.22) as

$$\phi = w + \varepsilon^{1/2}\phi_1 + \varepsilon\phi_2\,,$$

and equate powers of ε in (4.22). This yields the following problems for ϕ_1 and ϕ_2:

$$\lambda_0 w = L_1\phi_1 + L_2 w\,, \tag{4.25}$$

$$\lambda_1 w + \lambda_0\phi_1 = L_1\phi_2 + L_2\phi_1 + L_3 w\,. \tag{4.26}$$

To determine λ_0 and ϕ_1 we must formulate the appropriate solvability condition based on the adjoint operator L_1^* of L_1 defined by

$$L_1^*\phi \equiv L_0\phi - 2\frac{\int w^3\phi}{\int w^2}w\,. \tag{4.27}$$

Since L_1 admits a zero eigenvalue of multiplicity one, then so does L_1^*. In fact, w^* defined by

$$w^* \equiv (yw_y + w)/2\,, \tag{4.28}$$

is the unique element in the kernel of L_1^*, i.e. $L_1^*w^* = 0$, owing to the following two readily derived identities:

$$L_0w^* = w\,, \qquad 2\frac{\int w^3w^*}{\int w^2} = 1\,. \tag{4.29}$$

Next, we impose a solvability condition on (4.25) in the usual way. We multiply (4.25) by w^* and integrate by parts to derive that

$$\lambda_0 = \frac{\int w^*L_2w}{\int w^*w} = \left(c_0\int w^2 + c_1\int w^3\right)\frac{\int w^*w^3}{\int w^*w} = 2\left(c_0\int w^2 + c_1\int w^3\right)\,, \tag{4.30}$$

where we used the integral identity in (4.29) together with $\int w^* w = \int w^2/4$. From the formulae for the coefficients c_0 and c_1 in (4.24), (4.30) determines λ_0 as

$$\lambda_0 = \pm i\sqrt{\frac{\mu}{\tau_0}}\,. \tag{4.31}$$

Since λ_0 is purely imaginary, the next order term λ_1 needs to be computed to determine stability.

The problem (4.25) for ϕ_1 can be written by using (4.23 *a*) and (4.23 *b*) as

$$L_0\phi_1 = \lambda_0 w - \left(c_0\int w^2 + c_1\int w^3 + 2\frac{\int w\phi_1}{\int w^2}\right)w^3\,.$$

Since $L_0 w^* = w$ and $L_0 w = 2w^3$, we can write ϕ_1 as

$$\phi_1 = \lambda_0 w^* - \frac{dw}{2} \qquad \text{where} \qquad d \equiv c_0\int w^2 + c_1\int w^3 + 2\frac{\int w\phi_1}{\int w^2}\,. \tag{4.32}$$

Upon substituting ϕ_1 into the definition of d, we can then solve for d by using (4.30) for λ_0 to get

$$2d = c_0\int w^2 + c_1\int w^3 + 2\lambda_0\frac{\int ww^*}{\int w^2} = c_0\int w^2 + c_1\int w^3 + 2\left(c_0\int w^2 + c_1\int w^3\right)\frac{\int w^* w^3}{\int w^2}\,.$$

Finally, by using $\int w^* w = \int w^2/4$, the expression above simplifies to

$$d = c_0\int w^2 + c_1\int w^3$$

so that ϕ_1 is given explicitly from (4.32) as

$$\phi_1 = \left(c_0\int w^2 + c_1\int w^3\right)\left(2w^* - \frac{w}{2}\right)\,. \tag{4.33}$$

With ϕ_1 explicitly known, we impose the solvability condition on the problem (4.26) for ϕ_2 to determine λ_2 as

$$\lambda_1 = \frac{\int w^*\left(L_2 - \lambda_0\right)\phi_1 + \int w^* L_3 w}{\int w^* w}\,.$$

Upon using (4.33) for ϕ_1, $L_3 w$ from (4.23 *c*), and $(L_2 - \lambda_0)$ from (4.23 *b*), the integrals above are evaluated as

$$\begin{aligned}\lambda_1 = &\left(-\frac{16\pi^2}{9} - \frac{16}{3}\right)c_0^2 + \left(-\frac{4}{3}\sqrt{2}\pi - \frac{8}{9}\sqrt{2}\pi^3\right)c_1 c_0 - \frac{2\pi^4}{9}c_1^2\\ &+ \frac{\sqrt{2}\pi}{3}c_2 + \frac{3\sqrt{2}\pi}{5}c_4 + \frac{4\sqrt{2}\pi}{3}c_5 + 8c_6 + \frac{12\sqrt{2}\pi}{5}c_7 + 2\sqrt{2}c_8\pi + 2\sqrt{2}\pi c_9\,.\end{aligned}$$

Finally, upon substituting $c_0, \ldots, c_9$ from (4.24) into this expression, we determine λ_1 explicitly as

$$\lambda_1 = \frac{\alpha^2\pi^2}{2\mu^2} - \frac{\mu}{\tau_0}\left(\frac{24-\pi^2}{72}\right) \tag{4.34}$$

The two-term expansion for λ given in (4.14) follows from (4.31) and (4.34). The Hopf bifurcation threshold is obtained by setting $\lambda_1 = 0$. This occurs precisely as τ_0 is increased past τ_{0c}, where τ_c is given by (4.13). ■

5 Hot-Spot Patterns in 2-D: Equilibria and Stability

In this section we construct a K-spot quasi-steady-state solution to (1.1) in an arbitrary 2-D domain with spots centered at $x_1, \ldots, x_K$. To leading-order in $\sigma = -1/\log\varepsilon$, we then derive a threshold condition on the diffusivity D for the stability of the K-spot quasi-steady-state solution to instabilities that develop on an $\mathcal{O}(1)$ time-scale.

As in the analysis of hot-spot patterns in one spatial dimension, we set $V = P/A^2$ (see (2.2)) into (1.1) to obtain

$$A_t = \varepsilon^2 \Delta A - A + VA^3 + \alpha\,, \qquad x \in \Omega\,; \qquad \partial_n A = 0\,, \qquad x \in \partial\Omega\,, \tag{5.1 a}$$

$$\tau \left(A^2 V\right)_t = D\nabla \cdot \left(A^2 \nabla V\right) - VA^3 + \gamma - \alpha\,, \qquad x \in \Omega\,; \qquad \partial_n V = 0\,, \qquad x \in \partial\Omega\,. \tag{5.1 b}$$

We first motivate the ε-dependent re-scalings of V and A that are needed for the 2-D case. We suppose that $D \gg 1$, so that V is approximately constant. By integrating the steady-state equation of (5.1 b) over Ω we get $V = c/\int_\Omega A^3\,dx$, where c is some $\mathcal{O}(1)$ constant. Therefore, if $A = \mathcal{O}(\varepsilon^{-p})$ in the inner hot-spot region of area $\mathcal{O}(\varepsilon^2)$, we obtain $\int_\Omega A^3\,dx = \mathcal{O}(\varepsilon^{2-3p})$, so that $V = \mathcal{O}(\varepsilon^{3p-2})$. In addition, from the steady-state of (5.1 a), we must have in the inner region that $A^3V \sim A$, so that $-3p + (3p-2) = -p$. This yields $p = 2$. Therefore, for $D \gg 1$, $V = \mathcal{O}(\varepsilon^4)$ globally on Ω, while $A = \mathcal{O}(\varepsilon^{-2})$ in the inner region near a hot-spot. Finally, in the outer region we must have $A \sim \alpha = \mathcal{O}(1)$, so that from (5.1 b), we conclude that $D\nabla \cdot \left(A^2\nabla V\right) \sim \alpha - \gamma = \mathcal{O}(1)$. Since $V = \mathcal{O}(\varepsilon^4)$, this balance requires that $D = \mathcal{O}(\varepsilon^{-4})$. Finally, in the core of a hot-spot we conclude that the density P of criminals, given by $P = VA^2$, is $\mathcal{O}(1)$ as $\varepsilon \to 0$.

Although this simple scaling analysis correctly identifies the algebraic factors in ε, there are more subtle logarithmic terms of the form $\sigma \equiv -1/\log\varepsilon$ that are needed in the construction of the quasi-steady-state hot spot solution.

The scaling analysis above motivates the introduction of new variables v, u, and $\mathcal{D}$ defined by

$$V = \varepsilon^4 v\,, \qquad A = \varepsilon^{-2} u\,, \qquad D = \mathcal{D}/\varepsilon^4\,. \tag{5.2}$$

In terms of (5.2), (5.1) transforms exactly to

$$u_t = \varepsilon^2 \Delta u - u + vu^3 + \alpha\varepsilon^2\,, \qquad x \in \Omega\,; \qquad \partial_n u = 0\,, \qquad x \in \partial\Omega\,, \tag{5.3 a}$$

$$\tau \left(u^2 v\right)_t = \frac{\mathcal{D}}{\varepsilon^4}\nabla \cdot \left(u^2 \nabla v\right) - \varepsilon^{-2} vu^3 + \gamma - \alpha\,, \qquad x \in \Omega\,; \qquad \partial_n v = 0\,. \qquad x \in \partial\Omega\,. \tag{5.3 b}$$

Owing to the non-uniformity in the behavior as $|y| \to \infty$ of the solution to this core problem near a spot (see below), the construction of a quasi-steady-state K-spot solution for (5.3) is more intricate than that for the Gierer-Meinhardt, Schnakenburg, or Gray-Scott problems analyzed in [**39**]–[**44**], [**13**], [**16**], and [**1**]. As such, we will only develop a theory that is accurate to leading order in $\sigma \equiv -1/\log\varepsilon$, similar to that undertaken in [**39**]–[**44**], and [**13**]. This is in contrast to the recent approach in [**16**] and [**1**] that used a hybrid asymptotic-numerical method to construct quasi-steady-state spot patterns to the Schnakenburg and Gray-Scott systems, respectively, with an error that is beyond-all-orders with respect to σ.

In the outer region, away from the spots centered at $x_1, \ldots, x_K$, we expand u and v as

$$u = \alpha\varepsilon^2 + o(\varepsilon^2)\,, \qquad v \sim h_0 + \sigma h_1 + \cdots\,, \tag{5.4}$$

where $\sigma = -1/\log\varepsilon$ and $\mathcal{D} = \mathcal{D}_0/\sigma$, where $\mathcal{D}_0 = \mathcal{O}(1)$. From the steady-state of (5.3 b) we obtain that h_0 is constant, and that h_1 satisfies

$$\Delta h_1 = -\frac{(\gamma - \alpha)}{\alpha^2 \mathcal{D}_0}\,, \qquad x \in \Omega\backslash\{x_1, \ldots, x_K\}\,; \qquad \partial_n h_1 = 0\,, \qquad x \in \Omega\,. \tag{5.5}$$

As shown below, this problem must be augmented by certain singularity conditions that are obtained by matching the outer solution for v to certain inner solutions, one in the neighborhood of each spot.

In the inner region near the j-th spot centered at x_j we introduce the inner variables y, u_j, and v_j by

$$y = \varepsilon^{-1}(x - x_j)\,, \qquad v_j(y) = v(x_j + \varepsilon y)\,, \qquad u_j(y) = u(x_j + \varepsilon y)\,. \tag{5.6}$$

In terms of these inner variables, and with $\mathcal{D} = \sigma^{-1}\mathcal{D}_0$, the steady-state of (5.3) transforms exactly on $y \in \mathbb{R}^2$ to

$$\Delta_y u_j - u_j + v_j u_j^3 + \alpha\varepsilon^2 = 0\,, \tag{5.7 a}$$

$$\nabla_y \cdot \left(u_j^2 \nabla_y v_j\right) - \frac{\varepsilon^4\sigma}{\mathcal{D}_0} v_j u_j^3 = -\frac{\varepsilon^6\sigma}{\mathcal{D}_0}(\gamma - \alpha)\,, \tag{5.7 b}$$

where $\sigma \equiv -1/\log\varepsilon$. We will construct a radially symmetric solution $u_j = u_j(\rho)$, $v_j = v_j(\rho)$ to this problem, where $\rho = |y|$.

The complication in analyzing (5.7) is that $u_j = \mathcal{O}(1)$ for $|y| = \mathcal{O}(1)$, whereas $u_j = \mathcal{O}(\varepsilon^2)$ for $|y| \gg 1$. Therefore, the "diffusivity" u_j^2 in the operator for v in (5.7 *b*) ranges from $\mathcal{O}(1)$ when $|y| = \mathcal{O}(1)$ to $\mathcal{O}(\varepsilon^4)$ when $|y| \gg 1$. For this reason, we cannot simply neglect the second term on the left-hand side of (5.7 *b*) for all $|y|$. However, as we show below, we can neglect the $\mathcal{O}(\varepsilon^6)$ term on the right-hand side of (5.7 *b*).

For $|y| = \mathcal{O}(1)$, we expand u_j and v_j as

$$u_j = u_{j0} + \varepsilon^2 u_{j1} + \cdots\,, \qquad v_j = v_{j0} + \varepsilon^2 v_{j1} + \cdots\,. \tag{5.8}$$

Upon substituting this expansion into (5.7), we obtain that v_{j0} and v_{j1} are constants, and that u_{j0} and u_{j1} are radially symmetric solutions of

$$\Delta_\rho u_{j0} - u_{j0} + v_{j0} u_{j0}^3 = 0\,, \qquad \Delta_\rho u_{j1} - u_{j1} + 3u_{j0}^2 v_{j0} u_{j1} = -\alpha - u_{j0}^3 v_{j1}\,,$$

on $\rho \geq 0$ with $u_{j0} \to 0$ and $u_{j1} \to \alpha$ as $\rho \to \infty$. Here $\Delta_\rho g \equiv g'' + \rho^{-1} g'$ for $g = g(\rho)$. In terms of the unknown constants v_{j0} and v_{j1}, the solutions for u_{j0} and u_{j1} are

$$u_{j0} = v_{j0}^{-1/2} w\,, \qquad u_{j1} = \alpha - \frac{v_{j1}}{2v_{j0}^{3/2}} w - 3\alpha w_1\,, \tag{5.9}$$

where $w = w(\rho)$ and $w_1 = w_1(\rho)$ are the unique radially symmetric solutions of

$$\Delta_\rho w - w + w^3 = 0\,, \qquad L w_1 \equiv \Delta_\rho w_1 - w_1 + 3w^2 w_1 = w^2\,, \tag{5.10}$$

with $w(\rho) > 0$, $w'(0) = 0$, and $w \to 0$ as $\rho \to \infty$, together with $w_1'(0) = 0$ and $w_1 \to 0$ as $\rho \to \infty$. The expression (5.9) for u_{j1} shows that $u_{j1} \to \alpha$ as $\rho \to \infty$, so that from (5.8) $u_j \sim \alpha\varepsilon^2$ when $|y| \gg 1$.

Next, we calculate the far-field behavior, valid for $|y| \gg 1$, for the solution v_j to (5.7 *b*). To do so, we define the ball $\mathcal{B}_\delta = \{y \mid |y| \leq \delta\}$, where $1 \ll \delta \ll \mathcal{O}(\varepsilon^{-1})$. Therefore, this ball is defined in the intermediate matching region between the inner and outer scales y and x, respectively. Upon integrating (5.7 *b*) over $\mathcal{B}_\delta$, and using the divergence theorem, we obtain that

$$2\pi u_j^2 \delta v_j'|_{\rho=\delta} \sim \frac{\varepsilon^4\sigma}{\mathcal{D}_0} \int_{\mathcal{B}_\delta} v_j u_j^3\, dy + \mathcal{O}(\delta^2\sigma\varepsilon^6)\,. \tag{5.11}$$

Since $u_j = \mathcal{O}(1)$ only for $|y| = \mathcal{O}(1)$ where $v_j \sim v_{j0} + o(1)$, the integral on the right hand-side of (5.11) can be estimated by using $u_j \sim v_{j0}^{-1/2} w$. In contrast, on the left hand-side of (5.11) we use $u_j \sim \alpha\varepsilon^2$ on $\rho = \delta \gg 1$. In this way, we obtain that (5.11) becomes

$$2\pi\alpha^2\delta\varepsilon^4 v_j'|_{\rho=\delta} \sim \left(\frac{2\pi\varepsilon^4\sigma}{\sqrt{v_{j0}}\,\mathcal{D}_0}\right) \int_0^\infty w^3\, \rho\, d\rho + \mathcal{O}(\delta^2\sigma\varepsilon^6)\,. \tag{5.12}$$

Since $\delta \ll \mathcal{O}(\varepsilon^{-1})$, we can neglect the last term on the right hand-side of (5.12), which is equivalent to neglecting the right-hand side of (5.7 *b*) for the inner problem.

From (5.12) we obtain that the far-field behavior for $|y| \gg 1$ for the solution to (5.7 b) has the form

$$v_j \sim v_{j0} + \sigma \left(S_j \log |y| + \mathcal{O}(1) \right) , \tag{5.13 a}$$

where S_j is defined by

$$S_j \equiv \frac{b}{\alpha^2 \mathcal{D}_0 \sqrt{v_{j0}}} , \qquad b \equiv \int_0^\infty w^3 \rho \, d\rho . \tag{5.13 b}$$

Therefore, the appropriate core problem determining the asymptotic shape of the hot-spot profile is to seek a radially symmetric solution to

$$\Delta_y u_j - u_j + v_j u_j^3 + \alpha \varepsilon^2 = 0 , \qquad \nabla_y \cdot \left(u_j^2 \nabla_y v_j \right) = \frac{\varepsilon^4 \sigma}{\mathcal{D}_0} v_j u_j^3 . \tag{5.14}$$

The next step in the construction of the multi hot-spot quasi-steady-state pattern is to match the inner and outer solutions for v in order to determine v_{j0}. We let $y = \varepsilon^{-1}(x - x_j)$ in (5.13 a) to obtain that the outer solution for v must have the singularity behavior

$$v \sim v_{j0} + S_j + \sigma \left[S_j \log |x - x_j| + \mathcal{O}(1) \right] , \qquad \text{as} \quad x \to x_j , \quad j = 1, \ldots, K . \tag{5.15}$$

Upon comparing (5.15) with the outer expansion $v \sim h_0 + \sigma h_1 + \cdots$ from (5.4), we conclude that

$$h_0 = v_{j0} + S_j , \qquad j = 1, \ldots, K , \tag{5.16 a}$$

and that h_1 satisfies (5.5) subject to the singularity behaviors

$$h_1 \sim S_j \log |x - x_j| + \mathcal{O}(1) , \qquad \text{as} \quad x \to x_j , \quad j = 1, \ldots, K . \tag{5.16 b}$$

Upon using the divergence theorem, the problem for h_1 has a solution only when the solvability condition

$$\sum_{j=1}^K S_j = \frac{(\gamma - \alpha)}{2\pi \alpha^2 \mathcal{D}_0} |\Omega| , \tag{5.16 c}$$

is satisfied, where $|\Omega|$ is the area of Ω. When this condition is satisfied, the solution for h_1 can be written as

$$h_1 = -2\pi \sum_{i=1}^K S_i G(x; x_i) + \bar{h}_1 , \tag{5.17}$$

where $\bar{h}_1$ is a constant to be determined, and where $G(x; x_i)$ is the Neumann Green's function satisfying

$$\Delta G = \frac{1}{|\Omega|} - \delta(x - x_i) , \qquad x \in \Omega ; \qquad \partial_n G = 0 , \qquad x \in \partial\Omega , \tag{5.18 a}$$

$$\int_\Omega G(x; x_i) \, dx = 0 ; \qquad G \sim -\frac{1}{2\pi} \log |x - x_i| + \mathcal{O}(1) , \quad \text{as} \quad x \to x_i . \tag{5.18 b}$$

In summary, the asymptotic matching provides the following algebraic system for determining v_{j0} for $j = 1, \ldots, K$:

$$h_0 = \mathcal{F}(v_{j0}) \equiv v_{j0} + \frac{c}{\sqrt{v_{j0}}} , \qquad \sum_{j=1}^K v_{j0}^{-1/2} = \frac{|\Omega|(\gamma - \alpha)}{2\pi b} , \qquad c \equiv \frac{b}{\alpha^2 \mathcal{D}_0} . \tag{5.19}$$

A symmetric K-hot-spot quasi-steady-state solution corresponds to a solution of (5.19) for which $v_{j0} = v_0$ for all j. From (5.9), this solution is characterized by the fact that the hot-spot profile is, to leading-order, the same for each j. The result for such symmetric quasi-equilibria is summarized as follows:

Principal Result 5.1: *For $\varepsilon \to 0$, a symmetric K-hot-spot quasi-steady-state solution to (5.3) on the parameter*

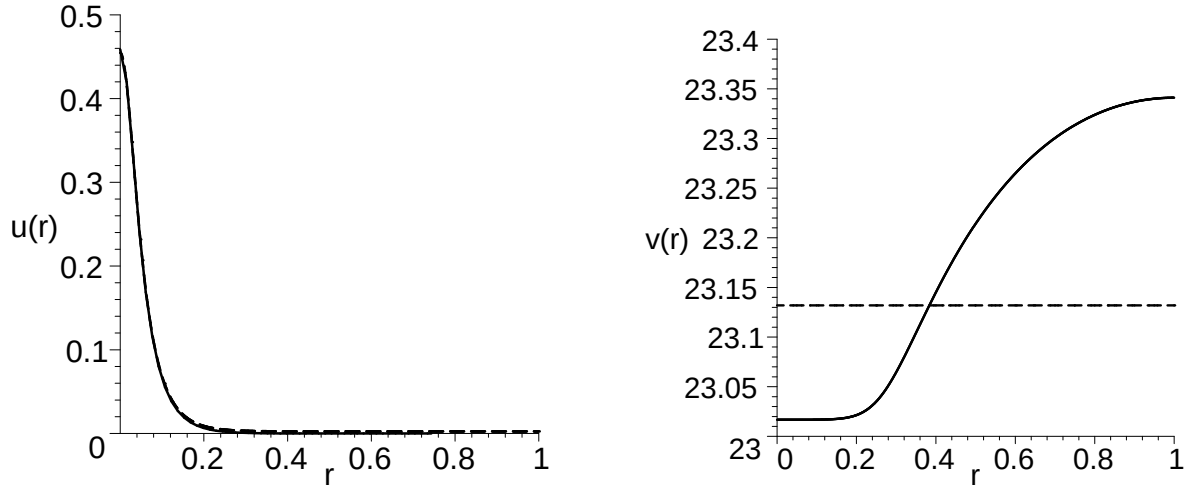

(*a*) (*b*)

Figure 6. Steady state hot-spot solution of (5.3) in a unit disk. Parameter values are $\varepsilon = 0.05, \alpha = 1, \gamma = 2, D = 500\varepsilon^{-2}, r = |x| < 1$. (a) The solid line is the steady state solution $u(r)$ of (5.3) computed by solving the associated radially symmetric boundary value problem numerically. The dashed line is the asymptotic approximation given by (5.20) (b) The solid line is the steady state solution for $v(r)$. Note the "flat knee" region within the spot center. The dashed line is the leading-order asymptotics $v \sim v_0$ given by (5.20).

regime $D = \varepsilon^{-4}\mathcal{D}_0/\sigma$ *with* $\sigma = -1/\log\varepsilon$*, is characterized as follows: In the inner region near the* j*-th hot-spot, where* $y = \varepsilon^{-1}(x - x_j)$*, then*

$$u \sim v_0^{-1/2} w + \mathcal{O}(\varepsilon^2)\,, \qquad v \sim v_0 + o(1)\,, \qquad v_0 \equiv \frac{4\pi^2 b^2 K^2}{|\Omega|^2(\gamma-\alpha)^2}\,, \tag{5.20}$$

where $b = \int_0^\infty w^3 \rho\, d\rho$*, and* $w(\rho)$ *with* $\rho = |y|$ *is the ground-state solution of (5.10). Alternatively, in the outer region where* $|x - x_j| \gg \mathcal{O}(\varepsilon)$ *for* $j = 1, \ldots, K$*, then*

$$u \sim \alpha\varepsilon^2\,, \qquad v \sim h_0 + \sigma h_1 + \cdots\,. \tag{5.21}$$

Here h_1 *is given in (5.17) in terms of the Neumann Green's function, and* h_0 *is a constant given by*

$$h_0 = v_0 + \frac{b}{\alpha^2\mathcal{D}_0\sqrt{v_0}} = \frac{4\pi^2 b^2 K^2}{|\Omega|^2(\gamma-\alpha)^2} + \frac{|\Omega|(\gamma-\alpha)}{2\pi\alpha^2 K\mathcal{D}_0}\,. \tag{5.22}$$

For a symmetric hot-spot pattern, the source strength S_j *in (5.17) is the same for each* j*, and is given in terms of* v_0 *by* $S_j = S_0 \equiv b/\left(\alpha^2\mathcal{D}_0\sqrt{v_0}\right)$ *where* $b \equiv \int_0^\infty w^3\rho\, d\rho$*.*

To illustrate Principal Result 5.1, we let Ω be the unit disk centered at the origin, and we choose $\alpha = 1, \gamma = 2, \varepsilon = 0.05$, and $D = 500\varepsilon^{-2}$. We consider a single hot-spot at the center of the disk. Upon numerically computing the ground-state solution w satisfying (5.10) we obtain that

$$w(0) \approx 2.2062\,, \qquad \int_{\mathbb{R}^2} w^3\, dy \approx 15.1097\,.$$

The asymptotic result (5.20) then yields

$$v_0 \sim \frac{(15.1097)^2}{(\gamma-\alpha)^2\pi^2} \approx 23.13184; \qquad u(0) \sim w(0)v_0^{-1/2} \approx 0.4587.$$

Alternatively, from the full numerical solution of the radially symmetric steady-state solution of (5.3), we compute that $v(0) \approx 23.017$ and $u(0) \approx 0.455$. The error is about 0.5% for $v(0)$ and about 0.8% for $u(0)$. A comparison of asymptotic and numerical results is shown in Fig. 6.

As a remark, the general shape of the function $\mathcal{F}(v)$ defined in (5.19) also shows that there can be asymmetric K-spot quasi-equilibria corresponding to spots of two distinct heights. Similar asymmetric patterns in 2-D have been constructed for the Gierer-Meihnardt and Gray-Scott systems in [**43**]) and ([**44**]. Let K_s and K_b be non-negative integers denoting the number of small and large spots, respectively, with $K = K_s + K_b$. Then, from (5.19), a K-spot asymmetric pattern is constructed by determining two distinct values v_{0s} and v_{0b} satisfying

$$\mathcal{F}(v_{0l}) = \mathcal{F}(v_{0r})\,, \qquad v_{0b} < v_{\min} < v_{0s}\,, \qquad \frac{K_s}{\sqrt{v_{0s}}} + \frac{K_b}{\sqrt{v_{0b}}} = \frac{|\Omega|(\gamma-\alpha)}{2\pi b}\,, \tag{5.23}$$

where $v_{\min} = 3\,(c/2)^{3/2}$ and c is defined in (5.19). The spatial profile of the hot-spot of large and small amplitude is given by $u \sim v_{0s}^{-1/2} w$ and $u \sim v_{0b}^{-1/2} w$, respectively.

We will not investigate the solvability with respect to $\mathcal{D}_0$ of the algebraic system (5.23) governing asymmetric spot patterns. Instead, in the next subsection we will study the stability properties of the symmetric K-hot-spot quasi-steady-state solution given in Principal Result 5.1.

5.1 The Stability of Hot-Spot Quasi-Steady-State Patterns

We linearize (5.3) around the quasi-steady-state K-hot-spot pattern to obtain the eigenvalue problem

$$\varepsilon^2 \Delta\phi - \phi + 3u^2 v\,\phi + u^3\,\psi = \lambda\phi\,, \qquad x \in \Omega\,; \qquad \partial_n \phi = 0\,, \qquad x \in \partial\Omega\,, \tag{5.24 a}$$

$$D\nabla\cdot\left(u^2\nabla\psi + 2u\phi\nabla v\right) - \frac{1}{\varepsilon^2}\left(3u^2 v\,\phi + u^3\,\psi\right) = \tau\lambda\left(u^2\psi + 2uv\phi\right)\,, \qquad x \in \Omega\,; \qquad \partial_n\psi = 0\,, \qquad x \in \partial\Omega\,. \tag{5.24 b}$$

In our stability analysis we will consider the range of D where $D = \varepsilon^{-4}\mathcal{D}_0/\sigma$ and $D_0 = \mathcal{O}(1)$. It is on this parameter range of D that a stability threshold occurs. Our main stability result is as follows:

Principal Result 5.2: *Consider the K-spot quasi-steady-state solution of (5.3) as constructed in Principal Result 5.1 for $\varepsilon \ll 1$. Assume that $\tau = \tau_0/\varepsilon^2$ where $\tau_0 = \mathcal{O}(1)$. Then, for $\varepsilon \to 0$, and to leading order in $\sigma = -1/\log\varepsilon$, the stability on an $\mathcal{O}(1)$ time-scale of a K-hot-spot quasi-steady-state solution with $K \geq 2$ is determined by the spectrum of the two distinct NLEP's*

$$\Delta_y \Phi - \Phi + 3w^2\Phi - \kappa_i w^3\left[\frac{\int_{\mathbb{R}^2} w^2\Phi\,dy}{\int_{\mathbb{R}^2} w^3\,dy} + \frac{2}{3}\tau_0\lambda\beta\frac{\int_{\mathbb{R}^2} w\Phi\,dy}{\int_{\mathbb{R}^2} w^2\,dy}\right] = \lambda\Phi\,, \qquad y \in \mathbb{R}^2\,, \tag{5.25 a}$$

with $\Phi \to 0$ as $|y| \to \infty$. Here κ_i for $i = 1, 2$ are defined by

$$\kappa_1 \equiv 3\,(1 + \tau_0\lambda\beta)^{-1}\,, \qquad \kappa_2 \equiv 3\left(1 + \tau_0\lambda\beta + \frac{\mathcal{D}_0}{2\mathcal{D}_{0c}}\right)^{-1}\,, \tag{5.25 b}$$

in terms of the constants β and $\mathcal{D}_{0c}$ defined by

$$\beta \equiv \frac{K\int_{\mathbb{R}^2} w^2\,dy}{|\Omega|(\gamma-\alpha)}\,, \qquad \mathcal{D}_{0c} \equiv \frac{|\Omega|^3\,(\gamma-\alpha)^3}{4\pi\alpha^2 K^3\left(\int_{\mathbb{R}^2} w^3\,dy\right)^2}\,. \tag{5.25 c}$$

For a one-hot-spot solution, for which $K = 1$, there is only a single NLEP with κ_i in (5.25 a) replaced by κ_1. For $\tau_0 \ll 1$, which is equivalent to $\tau \ll \mathcal{O}(\varepsilon^{-2})$, we conclude that a K-spot pattern with $K \geq 2$ is stable when $\mathcal{D}_0 < \mathcal{D}_{0c}$

and is unstable when $\mathcal{D}_0 > \mathcal{D}_{0c}$. In terms of the unscaled D, this yields the stability threshold

$$D = \left(\frac{\varepsilon^{-4}}{\sigma}\right)\mathcal{D}_{0c}\,, \quad \text{for} \quad K \geq 2\,, \qquad \sigma = -1/\log\varepsilon\,. \tag{5.26}$$

For $K = 1$ and $\tau_0 \ll 1$, a single hot-spot is stable for all $\mathcal{D}_0$ independent of ε.

To show that $\mathcal{D}_{0c}$ is the stability threshold of $\mathcal{D}_0$ for $K \geq 2$, we let $\tau_0 \to 0$ in (5.25) to obtain the limiting NLEP's

$$\Delta_y\Phi - \Phi + 3w^2\Phi - \kappa w^3\frac{\int_{\mathbb{R}^2} w^2\Phi\,dy}{\int_{\mathbb{R}^2} w^3\,dy} = \lambda\Phi\,, \qquad y \in \mathbb{R}^2\,; \qquad \Phi \to 0 \quad \text{as} \quad |y| \to \infty\,, \tag{5.27}$$

where κ can assume either of the two values

$$\kappa_{10} \equiv 3\,, \qquad \kappa_{20} \equiv 3\left(1 + \frac{\mathcal{D}_0}{2\mathcal{D}_{0c}}\right)^{-1}\,. \tag{5.28}$$

For (5.27), the rigorous result in Theorem 3 of [**45**] establishes the existence of an eigenvalue with $\mathrm{Re}(\lambda) > 0$ whenever $\kappa < 2$. Thus, since $\kappa_{20} < 2$ when $\mathcal{D}_0 > \mathcal{D}_{0c}$, we conclude that a K-hot-spot quasi-equilibria with $K > 2$ is unstable when $\mathcal{D}_0 > \mathcal{D}_{0c}$. In addition, the result in Theorem 1 of [**45**] (see the remark following Theorem 1) proves that all eigenvalues satisfy $\mathrm{Re}(\lambda) < 0$ when $2 < \kappa \leq 6$. Since $\kappa_{10} = 3$ and $2 < \kappa_{20} < 3$ for all $\mathcal{D}_0 < \mathcal{D}_{0c}$, it follows that the NLEP for a K-hot-spot quasi-steady-state solution with $K \geq 2$ does not have unstable eigenvalues when $\mathcal{D}_0 < \mathcal{D}_{0c}$. For $K = 1$, which corresponds to a one-hot-spot solution, the only choice for κ is $\kappa = \kappa_{10} = 3$, and so we have stability for any $\mathcal{D}_0 > 0$ independent of ε.

We make two remarks. Firstly, we anticipate that a single hot-spot solution where $K = 1$ will be stable provided that D_0 is not exponentially large in $1/\varepsilon$. The analysis to determine this stability threshold in the near-shadow limit should be similar to that done for the Gierer-Meinhardt model in [**14**]. Secondly, it is an open question to analyze (5.25) for $\tau_0 = \mathcal{O}(1)$ to determine if there are any Hopf bifurcations. The analysis of this problem in the 2-D context is much more difficult than in 1-D since the identity $L_0 w^2 = 3w^2$ for the local operator $L_0\Phi \equiv \Delta_y\Phi - \Phi + 3w^2\Phi$ in $\mathbb{R}^1$ no longer holds in $\mathbb{R}^2$. Moreover, since this identity does not hold in the 2-D case, we cannot determine λ explicitly when $\tau_0 \ll 1$ as was done for the 1-D case in Lemma 3.2.

The stability threshold in Principal Result 5.2 follows once we derive the NLEP (5.25). The derivation of this NLEP is done in several distinct steps.

We first consider the inner region near the j-th spot and we introduce the new variables y, $\Phi_j(y)$, and $\Psi_j(y)$ by

$$y = \varepsilon^{-1}(x - x_j)\,, \qquad \Phi_j(y) = \phi(x_j + \varepsilon y)\,, \qquad \Psi_j(y) = \psi(x_j + \varepsilon y)\,.$$

Then, with $D = \varepsilon^{-4}\mathcal{D}_0/\sigma$ and $\sigma = -1/\log\varepsilon$, (5.24) on $y \in \mathbb{R}^2$ becomes

$$\Delta_y\Phi_j - \Phi_j + 3u_j^2 v_j\,\Phi_j + u_j^3\,\Psi_j = \lambda\Phi_j\,, \tag{5.29 a}$$

$$\nabla_y\cdot\left(u_j^2\nabla_y\Psi_j + 2u_j\Phi_j\nabla_y v_j\right) - \frac{\varepsilon^4\sigma}{\mathcal{D}_0}\left(3u_j^2 v_j\,\Phi_j + u_j^3\,\Psi_j\right) = \frac{\tau\lambda\varepsilon^6\sigma}{\mathcal{D}_0}\left(u_j^2\Psi_j + 2u_j v_j\Phi_j\right)\,. \tag{5.29 b}$$

Since $u_j = \mathcal{O}(1)$ and $\nabla_y v_j = o(1)$ when $|y| = \mathcal{O}(1)$, we obtain from (5.29 b) that $\Psi_j = \Psi_{j0} + \mathcal{O}(\varepsilon^2)$ when $|y| = \mathcal{O}(1)$, where Ψ_{j0} is an unknown constant. Then, with $u_j \sim w/\sqrt{v_0}$ and $v_j \sim v_0$ for $|y| = \mathcal{O}(1)$, we obtain from (5.29 a) that $\Phi_j \sim \Phi_{j0} + o(1)$, where Φ_{j0} satisfies

$$\Delta_y\Phi_{j0} - \Phi_{j0} + 3w^2\Phi_{j0} + v_0^{-3/2}w^3\,\Psi_{j0} = \lambda\Phi_{j0}\,, \qquad y \in \mathbb{R}^2\,; \qquad \Phi_{j0} \to 0 \quad \text{as} \quad |y| \to \infty\,, \tag{5.30}$$

where w is the radially symmetric ground-state solution satisfying (5.10).

The next step in the analysis is to determine the constant Ψ_{j0} in (5.30). This is done by first determining the far-field behavior as $|y| \to \infty$ of the solution to (5.29 b). We define the ball $\mathcal{B}_\delta = \{y \mid |y| \le \delta\}$, where $1 \ll \delta \ll \mathcal{O}(\varepsilon^{-1})$, and we integrate (5.29 b) over $\mathcal{B}_\delta$ to obtain

$$\left(2\pi u_j^2 \Psi_j'|_{\rho=\delta} + 4\pi u_j \Phi_j v_j'|_{\rho=\delta}\right)\delta = \frac{\varepsilon^4\sigma}{\mathcal{D}_0}\int_{\mathcal{B}_\delta}\left(\Psi_j u_j^3 + 3u_j^2 v_j \Phi_j\right)\,dy + \frac{\tau\lambda\varepsilon^6\sigma}{\mathcal{D}_0}\int_{\mathcal{B}_\delta}\left(\Psi_j u_j^2 + 2u_j v_j \Phi_j\right)\,dy\,. \tag{5.31}$$

We now estimate the terms in (5.31) for $\varepsilon \ll 1$.

Since the dominant contribution to the integrals on the right hand-side of (5.31) arises from the region where $|y| = \mathcal{O}(1)$, we can asymptotically estimate these integrals by using $u_j \sim w/\sqrt{v_0}$, $v_j \sim v_0$, and $\Psi_j \sim \Psi_{j0}$. For the left hand-side of (5.31) we use $u_j \sim \alpha\varepsilon^2$ on $\rho \equiv |y| = \delta \gg 1$ to get

$$\left(2\pi\varepsilon^4\alpha^2\Psi_j'|_{\rho=\delta} + 4\pi\varepsilon^2\alpha v_j'\Phi_j|_{\rho=\delta}\right)\delta \sim \frac{\varepsilon^4\sigma}{\mathcal{D}_0}\left[\frac{\Psi_{j0}}{v_0^{3/2}}\int_{\mathbb{R}^2} w^3\,dy + 3\int_{\mathbb{R}^2} w^2\Phi_{j0}\,dy\right] + \frac{\tau\lambda\varepsilon^6\sigma}{\mathcal{D}_0}\left[\frac{\Psi_{j0}}{v_0}\int_{\mathbb{R}^2} w^2\,dy + 2\sqrt{v_0}\int_{\mathbb{R}^2} w\Phi_{j0}\,dy\right]. \tag{5.32}$$

Next, we estimate the second term on the left hand-side of (5.32). For $|y| \gg 1$, we obtain from the outer limit of (5.29 a) that $-\Phi_j + \varepsilon^3\alpha^6\Psi_j \sim \lambda\Phi_j$, so that with $\Psi_j \sim \Psi_{j0} + o(1)$, we get

$$\Phi_j \sim \frac{\varepsilon^6\alpha^3}{1+\lambda}\Psi_{j0}\,, \qquad \text{on} \quad \rho = |y| = \delta \gg 1\,. \tag{5.33}$$

In addition, from (5.13 a), we estimate that $v_j'|_{\rho=\delta} \sim \sigma S_0/\delta$, where S_0 is defined in Principal Result 5.1. Substituting this estimate together with (5.33) into (5.32) we obtain

$$\Psi_j'|_{\rho=\delta}\delta + \frac{2\alpha^2\varepsilon^4\sigma S_0}{(1+\lambda)}\Psi_{j0} \sim \frac{\sigma}{2\pi\mathcal{D}_0\alpha^2}\left[\frac{\Psi_{j0}}{v_0^{3/2}}\int_{\mathbb{R}^2} w^3\,dy + 3\int_{\mathbb{R}^2} w^2\Phi_{j0}\,dy\right] + \frac{\tau\lambda\varepsilon^2\sigma}{2\pi\mathcal{D}_0\alpha^2}\left[\frac{\Psi_{j0}}{v_0}\int_{\mathbb{R}^2} w^2\,dy + 2\sqrt{v_0}\int_{\mathbb{R}^2} w\Phi_{j0}\,dy\right]. \tag{5.34}$$

From (5.34), and under the assumption that $\tau = \varepsilon^{-2}\tau_0$, where $\tau_0 = \mathcal{O}(1)$, we conclude that Ψ_j has the far-field behavior

$$\Psi_j \sim \Psi_{j0} + \sigma\left(B_j \log|y| + \mathcal{O}(1)\right)\,, \qquad \text{for} \quad |y| \gg 1\,, \tag{5.35}$$

where B_j for $j = 1, \ldots, K$ is defined by

$$B_j \sim \frac{1}{2\pi\mathcal{D}_0\alpha^2}\left[\frac{\Psi_{j0}}{v_0^{3/2}}\int_{\mathbb{R}^2} w^3\,dy + 3\int_{\mathbb{R}^2} w^2\Phi_{j0}\,dy\right] + \frac{\tau_0\lambda}{2\pi\mathcal{D}_0\alpha^2}\left[\frac{\Psi_{j0}}{v_0}\int_{\mathbb{R}^2} w^2\,dy + 2\sqrt{v_0}\int_{\mathbb{R}^2} w\Phi_{j0}\,dy\right]. \tag{5.36}$$

Upon writing (5.35) in terms of the outer variable $(x - x_j) = \varepsilon y$, we obtain that the matching condition for the outer solution ψ is

$$\psi \sim B_j + \Psi_{j0} + \sigma\left(B_j \log|x - x_j| + \mathcal{O}(1)\right)\,, \qquad \text{as} \quad x \to x_j\,, \quad j = 1, \ldots, K\,. \tag{5.37}$$

Next, we consider the outer region for ψ where $|x - x_j| = \mathcal{O}(1)$ for $j = 1, \ldots, K$. In (5.24 b) we use $u \sim \alpha\varepsilon^2$, $\nabla v = \mathcal{O}(\sigma)$, and $\phi = \mathcal{O}(\varepsilon^6)$ from (5.33) to estimate that

$$\frac{\mathcal{D}_0}{\sigma\varepsilon^4}\nabla\cdot\left(\alpha^2\varepsilon^4\nabla\psi + \mathcal{O}(\sigma\varepsilon^8)\right) - \varepsilon^{-2}\left(\alpha^3\varepsilon^6\psi + \mathcal{O}(\sigma\varepsilon^{10})\right) = \tau\lambda\left(\alpha^2\varepsilon^4\psi + \mathcal{O}(\sigma\varepsilon^8)\psi\right)\,.$$

Hence, when $\tau = \varepsilon^{-2}\tau_0$ we obtain that $\mathcal{D}_0\Delta\psi \sim \tau_0\lambda\varepsilon^2\sigma\psi$. In order to match with (5.37) we must expand the outer

solution for ψ as

$$\psi = \psi_0 + \sigma\psi_1 + \cdots . \tag{5.38}$$

We then obtain that ψ_0 is a constant, given by

$$\psi_0 = \Psi_{j0} + B_j \,, \qquad j = 1, \ldots, K \,, \tag{5.39}$$

and that ψ_1 satisfies

$$\Delta\psi_1 = 0 \,, \qquad x \in \Omega \backslash \{x_1, \ldots, x_K\} \,; \qquad \partial_n \psi_1 = 0 \,, \quad x \in \partial\Omega \,, \tag{5.40 a}$$

$$\psi_1 \sim B_j \log|x - x_j| + \mathcal{O}(1) \,, \qquad \text{as} \quad x \to x_j \,, \quad j = 1, \ldots, K \,. \tag{5.40 b}$$

The solvability condition for (5.40) is that $\sum_{j=1}^{K} B_j = 0$. Upon summing (5.39) from $j = 1, \ldots, K$, we obtain that

$$B_j = -\Psi_{j0} + \frac{1}{K} \sum_{j=1}^{K} \Psi_{j0} \,, \tag{5.41}$$

where B_j is given in (5.36).

The final step in the derivation of the NLEP is to solve (5.36) and (5.41) for Ψ_{j0} and substitute the resulting expression into (5.30). To do so, We introduce the vectors $\mathcal{B} \equiv (B_1, \ldots, B_K)^T$ and $\hat{\Psi} \equiv (\Psi_{01}, \ldots, \Psi_{0K})^T$, and we write the system (5.36) and (5.41) in matrix form as

$$\mathcal{B} = c_1 \hat{\Psi}_0 - c_2 \mathcal{F}_0 + c_3 \hat{\Psi}_0 - c_4 \mathcal{F}_1 \,, \qquad \mathcal{B} = -\left(I - \mathcal{E}\right) \hat{\Psi}_0 \,, \tag{5.42}$$

where the constants c_i for $i = 1, \ldots, 4$ are defined by

$$c_1 \equiv \frac{1}{2\pi \mathcal{D}_0 \alpha^2 v_0^{3/2}} \int_{\mathbb{R}^2} w^3 \, dy \,, \qquad c_2 \equiv 3 c_1 v_0^{3/2} \,, \qquad c_3 \equiv \frac{\tau_0 \lambda}{2\pi \mathcal{D}_0 \alpha^2 v_0} \int_{\mathbb{R}^2} w^2 \, dy \,, \qquad c_4 \equiv 2 v_0^{3/2} c_3 \,, \tag{5.43 a}$$

and the vectors $\mathcal{F}_0$ and $\mathcal{F}_1$ are defined by

$$\mathcal{F}_0 \equiv -\frac{\int_{\mathbb{R}^2} w^2 \hat{\Phi}_0 \, dy}{\int_{\mathbb{R}^2} w^3 \, dy} \,, \qquad \mathcal{F}_1 \equiv -\frac{\int_{\mathbb{R}^2} w \hat{\Phi}_0 \, dy}{\int_{\mathbb{R}^2} w^2 \, dy} \,. \tag{5.43 b}$$

Here $\hat{\Phi}_0 \equiv (\Phi_{01}, \ldots, \Phi_{0K})^T$. In (5.42), I is the $K \times K$ identity matrix and the matrix $\mathcal{E}$ is defined by $\mathcal{E} = K^{-1} e e^T$, where $e \equiv (1, \ldots, 1)^T$.

By solving (5.42) for $\hat{\Psi}_0$, and substituting the resulting expression into (5.30), we obtain the vector NLEP

$$\Delta_y \hat{\Phi}_0 - \hat{\Phi}_0 + 3 w^2 \hat{\Phi}_0 + w^3 \mathcal{M} \left(\mathcal{F}_0 + \frac{c_4}{c_2} \mathcal{F}_1 \right) = \lambda \hat{\Phi}_0 \,, \tag{5.44}$$

where the matrix $\mathcal{M}$ is defined by

$$\mathcal{M} \equiv v_0^{-3/2} \left[\frac{(1 + c_1 + c_3)}{c_2} I - \frac{1}{c_2} \mathcal{E} \right]^{-1} . \tag{5.45}$$

The matrix $\mathcal{M}^{-1}$ is a rank-one update of a scalar multiple of the identity matrix. As such, its spectrum $\mathcal{M}\omega = \kappa\omega$ can readily be calculated as

$$\kappa_1 = \frac{c_2}{(c_1 + c_3) v_0^{3/2}} \,, \quad \omega_1 = (1, \ldots, 1)^T \,; \qquad \kappa_2 = \ldots = \kappa_K = \frac{c_2}{(1 + c_1 + c_3) v_0^{3/2}} \,, \quad \omega_j^T e = 0 \,, \quad j = 2, \ldots, K \,.$$

Notice that the eigenvectors corresponding to the matrix eigenvalues κ_j for $j = 2, \ldots, K$ span the $K - 1$ dimensional subspace perpendicular to $e = (1, \ldots, 1)^T$. As such, the *competition instability modes* correspond to $j = 2, \ldots, K$, whereas the synchronous instability mode corresponds to κ_1 with eigenvector $\omega_1 = (1, \ldots, 1)^T$.

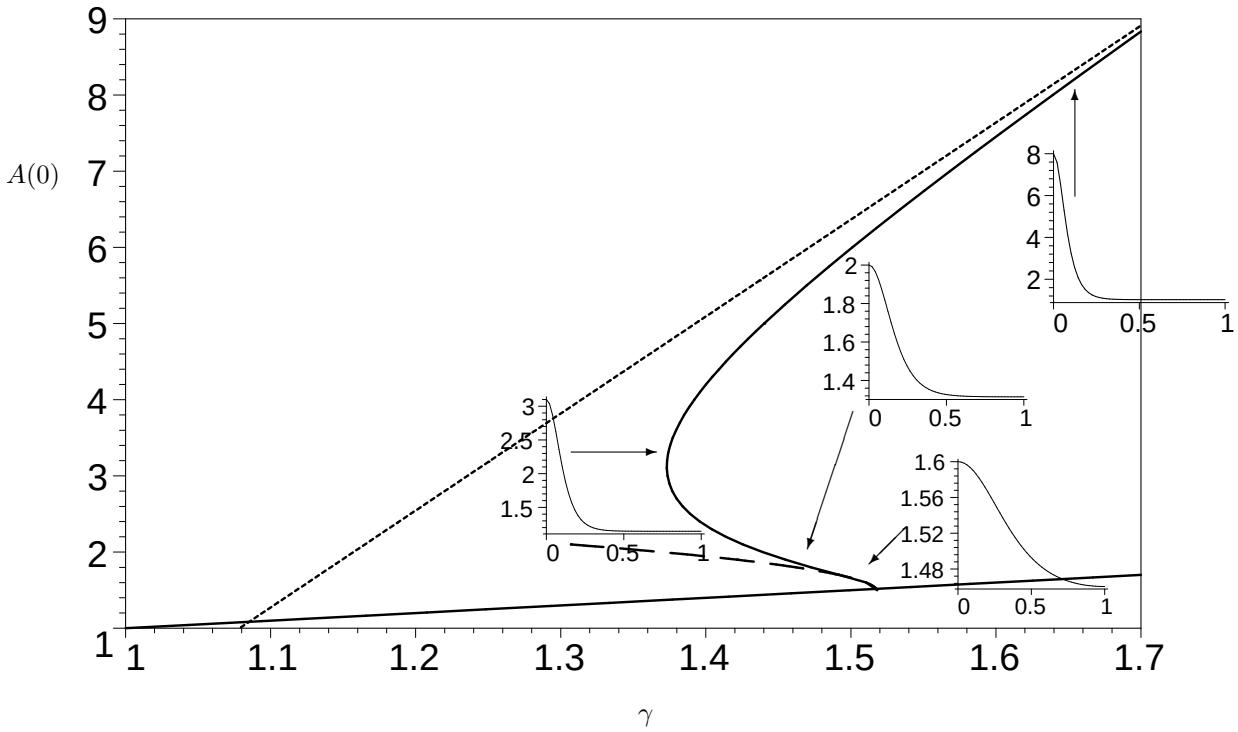

Figure 7. Numerically computed bifurcation diagram of $A(0)$ vs. γ. The parameter values are $\alpha = 1, \varepsilon = 0.05, x \in [0,1]$, and $D = 2$. A localized hot-spot appears for large values of $A(0)$. The asymptotics $A(0) \sim \frac{2(\gamma-\alpha)}{\varepsilon\pi}$ (see (2.19)) are shown by a dotted line. The constant steady state $A \sim \gamma$ is indicated by a solid straight line line. Turing patterns are born from the spatially uniform steady state as a result of a Turing bifurcation at $\gamma \sim 3\alpha/2 = 1.5$. The weakly nonlinear regime is indicated by a dashed parabola coming out of the bifurcation point. Inserts shows the change in the shape of the profile $A(x)$ along the bifurcation curve.

Then, we use the explicit formulae for c_j in (5.43 *a*) and for v_0 in (5.20) to write κ_i for $i = 1, 2$ as in (5.25 *b*). In addition, the ratio c_4/c_2 in (5.44) can be calculated using (5.43 *a*) and (5.20) to get $c_4/c_2 = 2\tau_0\lambda\beta/3$, where β is defined in (5.25 *c*). Finally, by diagonalizing the vector NLEP (5.44) by using the matrix decomposition of $\mathcal{M}$, and by recalling the definition of $\mathcal{F}_i$ for $i = 0, 1$ in (5.43 *b*), we obtain the NLEP (5.25) of Principal Result 5.2. This completes the derivation of Principal Result 5.2 ■.

5 Discussion

We have studied localized hot-spot solutions of (1.1) in one and two spatial dimensions in the regime $\varepsilon^2 \ll 1$ with $D \gg 1$. In this large D limit, steady-state multi hot-spot solutions have been constructed and their stability properties investigated with respect to D and τ from the analysis of certain nonlocal eigenvalue problems. An open problem is to characterize the dynamics of multi hot-spot patterns by reducing (1.1) to a finite dimensional dynamical system for the locations of the hot-spots in a quasi-steady-state pattern as was done for various two-component reaction-diffusion models without drift terms in [**6**, **7**, **9**, **33**, **16**, **1**].

We now remark on how the localized states constructed in this paper are related to the weakly nonlinear Turing patterns studied in [**29**, **30**, **31**]. In contrast to the theory developed in [**30**, **31**], our parameter values for (1.1) are not restricted to lie close to the Turing bifurcation point. In the limit $\varepsilon \to 0$, the spatially homogeneous steady-state

solution for (1.1) is $A_e = \gamma$ and $P_e = (\gamma - \alpha)/\gamma$. For $\varepsilon \to 0$, it is linearly unstable when (see equation (2.8) of [**30**])

$$\gamma > \frac{3}{2}\alpha\,, \qquad \text{as} \qquad \varepsilon \to 0\,,$$

and a spatially heterogeneous solution bifurcates off the homogeneous steady state at $\gamma \sim \frac{3}{2}\alpha$ as $\varepsilon \to 0$. In contrast, a localized hot-spot exists for the wider parameter range $\gamma > \alpha$. In Fig. 7 we plot the numerically computed bifurcation diagram for $A(0)$ vs. γ on a one-dimensional interval, with other parameters as indicated in the figure caption. The Turing bifurcation at $\gamma = \frac{3}{2}\alpha$ is subcritical when $\varepsilon \ll 1$ (cf. [**30**]), which is consistent with the stability of the constant state when $\gamma < \frac{3}{2}\alpha$. However, the bifurcation curve quickly turns around as it enters the localized regime. This is consistent with the existence of localized states when $\gamma > \alpha$.

The dispersion relation obtained by linearizing (1.1) about the spatially uniform state A_e, P_e is calculated as

$$\tau\lambda^2 + \lambda\left(A_e + Dm^2 + \tau(1-P_e) + \tau\varepsilon^2 m^2\right) + A_e(1+\varepsilon m^2) - 3DP_e m^2 + Dm^2(1+\varepsilon^2 m^2) = 0\,, \tag{5.1}$$

where $A_e = \gamma$ and $P_e = (\gamma - \alpha)/\gamma$. For $\gamma > \frac{3}{2}\alpha$, it is readily shown from this relation that the edges of the Turing instability band $m_{\rm lower} < m < m_{\rm upper}$ satisfy

$$m_{\rm lower} \sim D^{-1/2}\gamma(2\gamma - 3\alpha)^{-1/2}\,; \qquad m_{\rm upper} \sim \varepsilon^{-1}\gamma^{-1/2}(2\gamma - 3\alpha)^{1/2}\,, \qquad \text{as} \;\; \varepsilon \to 0\,.$$

The most unstable mode (i.e. the one which grows the fastest, and therefore the one most commonly observed) is obtained by setting $d\lambda/dm = 0$ in (5.1). For $\varepsilon \to 0$, this gives the maximum growth rate

$$\lambda_{\rm dominant} \sim 3P_e - 1 - 2\varepsilon^2 m^2\,,$$

together with the most unstable mode

$$m_{\rm dominant} \sim \varepsilon^{-1/2} D^{-1/4}\gamma^{-1/2}\left[(\gamma-\alpha)(3\gamma^2 + 2\tau(2\gamma - 3\alpha)\right]^{1/4}\,,$$

which is consistent with [**29**] in the limit $\varepsilon \to 0$ (see also equation (2.9) of [**30**]).

Correspondingly, this implies that for an initial condition consisting of a random perturbation of the spatially uniform steady-state, the preferred pattern has a characteristic half-length $l_{\rm turing} \sim \pi/m_{\rm dominant}$, where

$$l_{\rm turing} \sim \varepsilon^{1/2} D^{1/4}\gamma^{1/2}\left[(\gamma-\alpha)(3\gamma^2 + 2\tau(2\gamma - 3\alpha))\right]^{-1/4}\pi\,.$$

In contrast, for localized structures the characteristic length l between hot-spots to ensure stability of a multi hot-spot pattern, as obtained from (1.4), is that $l > l_c$ where

$$l_c \sim \sqrt{\pi} D^{1/4}\varepsilon^{1/2}\alpha^{1/2}(\gamma - \alpha)^{-3/4}\,. \tag{5.2}$$

Although $l_{\rm turing}$ and l_c are not related, they are both of the same asymptotic order $O(D^{1/4}\varepsilon^{1/2})$, which implies that the number of stable localized hot-spots corresponds roughly to the most unstable Turing mode. In fact, for a large parameter range, the inequality $l_c < l_{\rm turing}$ holds. For example, when $\tau = 1, \alpha = 1, \gamma = 2$ we calculate that $l_c/l_{\rm turing} = 0.7 < 1$. This was already observed empirically in Fig. 6 of [**29**].

Formula (1.4) provides an upper bound K_c on the number K of stable hot-spots in the regime where $D \gg 1$. On the other hand, numerical evidence shows the existence of a *lower bound* that occurs when D is sufficiently small. In this regime an instability occurs when there are *too few* hot-spots. In fact, if the hot-spot inter-distance exceeds some critical length, then a hot-spot insertion phenomena is observed (see Fig. 8). From Fig. 8, it appears that hot-spot insertion takes place every time that D is quartered. A similar insertion phenomenon occurs in other reaction-diffusion systems such as a chemotaxis model [**26**], the Gray-Scott model [**27**], the ferrocyanide-iodide-sulfite

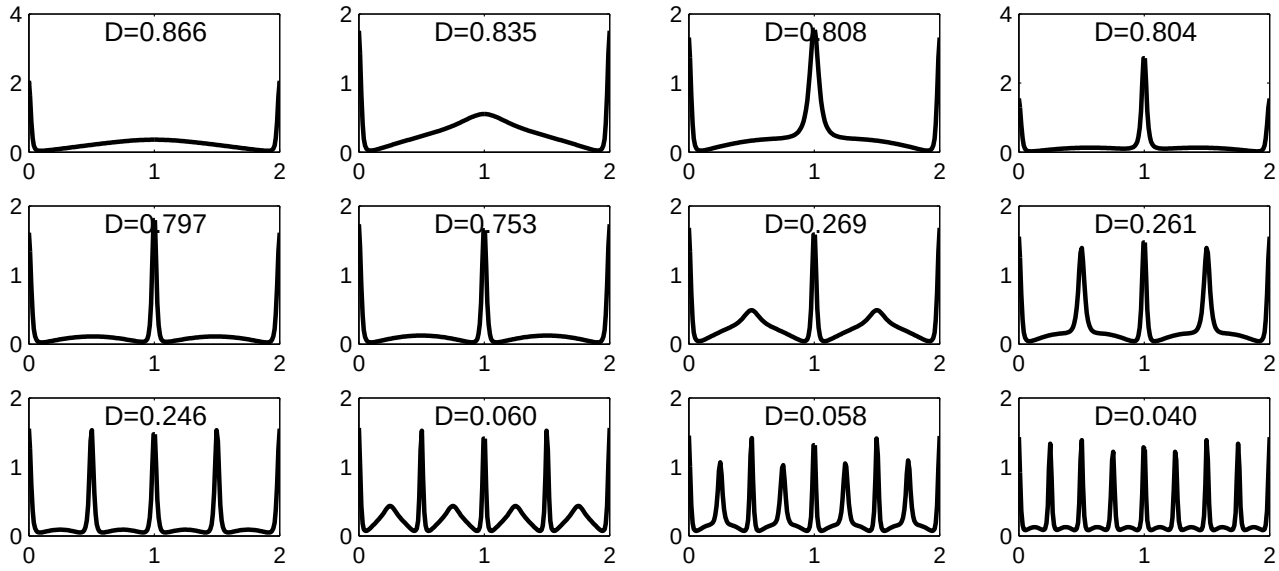

Figure 8. Hot-spot insertion phenomenon. Numerical solution of (1.1) with $\varepsilon = 0.02, \alpha = 1, \gamma = 2, D = 1/(1 + 0.01t)$ with $x \in (0, 2)$. Initial conditions consist of two boundary hot-spots. Snapshots of $P(x)$ are shown for values of D as indicated. Hot-spot insertion takes place every time that D is quartered.

system [**20**], the Brusselator [**17**], the Schnakenburg model [**16**], and a model of droplet breakup [**21**]. The detailed analysis of hot-spot insertion phenomena in (1.1) will be considered in future work.

Acknowledgements

T. K. and M. J. W. were supported by NSERC Discovery Grants (Canada). J. W. was supported from an Earmarked Grant of the RGC of Hong Kong.

References

[1] W. Chen and M. J. Ward (2009), *Oscillatory instabilities and dynamics of multi-spike patterns for the one-dimensional Gray-Scott model*, Europ. J. Appl. Math **20**(2), pp. 187–214.

[2] W. Chen and M. J. Ward (2011), *The stability and dynamics of localized spot patterns in the two-dimensional Gray-Scott model*, SIAM J. Appl. Dyn. Sys., **10**(2), (2011), pp. 582–666.

[3] A. Doelman, R. A. Gardner and T. J. Kaper (2001), *Large stable pulse solutions in reaction-diffusion equations*, Indiana U. Math. J., **50**(1), pp. 443–507.

[4] A. Doelman, R. A. Gardner and T. J. Kaper (2002), *A stability index analysis of 1-D patterns of the Gray Scott model*, Memoirs of the AMS, **155**, No. 737.

[5] A. Doelman, R. A. Gardner and T. J. Kaper (1998), *Stability analysis of singular patterns in the 1D Gray-Scott model: A matched asymptotic approach*, Physica D, **122**(1-4), pp. 1–36.

[6] A. Doelman and T. J. Kaper (2003), *Semistrong pulse interactions in a class of coupled reaction-diffusion systems*, SIAM J. Appl. Dyn. Sys., **2**(1), pp. 53–96.

[7] A. Doelman, T. J. Kaper and K. Promislow (2007), *Nonlinear asymptotic stability of the semi-strong pulse dynamics in a regularized Gierer-Meinhardt model*, SIAM J. Math. Anal., **38**(6), pp. 1760–1789.

[8] T. Hillen and A. Potapov (2004), *The one-dimensional chemotaxis model: global existence and asymptotic profile*, Math. Meth. Appl. Sci., **27**, pp. 1783–1801.

[9] D. Iron and M. J. Ward (2002), *The dynamics of multi-spike solutions to the one-dimensional Gierer-Meinhardt model*, SIAM J. Appl. Math., **62**(6), pp. 1924–1951.

[10] D. Iron, M. J. Ward and J. Wei (2001), *The stability of spike solutions to the one-dimensional Gierer-Meinhardt model*, Physica D, **150**(1-2), pp. 25–62.

[11] D. Iron, J. Wei and M. Winter (2004), *Stability analysis of Turing patterns generated by the Schnakenberg model*, J. Math. Biol., **49**(4), pp. 358–390.

[12] K. Kang, T. Kolokolnikov and M. J. Ward (2007), *The stability and dynamics of a spike in a one-dimensional Keller-Segel model*, IMA J. Appl. Math., **72**(2), pp. 140–162.

[13] T. Kolokolnikov and M. J. Ward (2003), *Reduced-wave Green's functions and their effect on the dynamics of a spike for the Gierer-Meinhardt model*, Europ. J. Appl. Math., **14**(5), pp. 513–545.

[14] T. Kolokolnikov and M. J. Ward (2004), *Bifurcation of spike equilibria in a near shadow reaction-diffusion System*, DCDS-B, **4**(4), pp. 1033–1064.

[15] T. Kolokolnikov, M. J. Ward and J. Wei (2005), *The existence and stability of spike equilibria in the one-dimensional Gray-Scott model: The low feed-rate regime*, Studies in Appl. Math., **115**(1), pp. 21–71.

[16] T. Kolokolnikov, M. J. Ward and J. Wei (2009), *Spot self-replication and dynamics for the Schnakenburg model in a two-dimensional domain*, J. Nonlinear Sci., **19**(1), pp. 1–56.

[17] T. Kolokolnikov, M. J. Ward, and J. Wei (2007), *Self-replication of mesa patterns in reaction-diffusion models*, Physica D, **236**(2), pp. 104–122.

[18] T. Koloklonikov, M. J. Ward and J. Wei (2006), *Slow translational instabilities of spike patterns in the one-dimensional Gray-Scott model*, Interfaces and Free Boundaries, **8**(2), pp. 185–222.

[19] T. Kolokolnikov and J. Wei (2011), *Stability of spiky solutions in a competition model with cross-diffusion*, SIAM J. Appl. Math. **71**, pp. 1428–1457.

[20] K. J. Lee and H. L. Swinney (1995), *Lamellar structures and self-replicating spots in a reaction-diffusion systems*, Phys. Rev. E., **51**(3), pp. 1899–1915.

[21] W. Liu, A. L. Bertozzi, and T. Kolokolnikov (2012), *Diffuse interface surface tension models in an expanding flow*, Comm. Math. Sci., **10**(1), pp. 387–418.

[22] R. McKay and T. Kolokolnikov (2012), *Stability transitions and dynamics of localized patterns near the shadow limit of reaction-diffusion systems*, to appear, DCDS-B.

[23] C. B. Muratov and V. V. Osipov (2002), *Stability of static spike autosolitons in the Gray-Scott model*, SIAM J. Appl. Math., **62**(5), pp. 1463–1487.

[24] C. B. Muratov and V. V. Osipov (2000), *Static spike autosolitons in the Gray-Scott model*, J. Phys. A: Math Gen., **33**, pp. 8893–8916.

[25] Y. Nishiura (2002), *Far-from equilibrium dynamics, translations of mathematical monographs*, Vol. **209**, AMS Publications, Providence, Rhode Island.

[26] K. Painter and T. Hillen (2011), *S*patio-temporal chaos in a chemotaxis Model, Physica D, **240**, pp. 363–375.

[27] J. E. Pearson (1993), *Complex Patterns in a Simple System*, Science, **216**, pp. 189–192.

[28] A. Potapov and T. Hillen (2005), *Metastability in chemotaxis models*, J. Dynam. Diff. Eq., **17**(2) pp. 293-330.

[29] M. B. Short, M. R. D'Orsogna, V. B. Pasour, G. E. Tita, P. J. Brantingham, A. L. Bertozzi and L. B. Chayes (2008), *A statistical model of criminal behavior*, Math. Models. Meth. Appl. Sci., **18**, Suppl. pp. 1249–1267.

[30] M. B. Short, A. L. Bertozzi and P. J. Brantingham (2010), *Nonlinear patterns in urban crime - hotpsots, bifurcations, and suppression*, SIAM J. Appl. Dyn. Sys., **9**(2), pp. 462–483.

[31] M. B. Short, P. J. Brantingham, A. L. Bertozzi and G. E. Tita (2010), *Dissipation and displacement of hotpsots in reaction-diffusion models of crime*, Proc. Nat. Acad. Sci. **107**(9) pp. 3961-3965.

[32] B. Sleeman, M. J. Ward and J. Wei (2005), *The existence and stability of spike patterns in a chemotaxis model*, SIAM J. Appl. Math., **65**(3), pp. 790–817.

[33] W. Sun, M. J. Ward and R. Russell (2005), *The slow dynamics of two-spike solutions for the Gray-Scott and Gierer-Meinhardt systems: competition and oscillatory instabilities*, SIAM J. Appl. Dyn. Syst., **4**(4), pp. 904–953.

[34] H. Van der Ploeg and A. Doelman (2005), *Stability of spatially periodic pulse patterns in a class of singularly perturbed reaction-diffusion equations*, Indiana Univ. Math. J., **54**(5), p. 1219-1301.

[35] M. J. Ward and J. Wei (2003), *Hopf bifurcations and oscillatory instabilities of spike solutions for the one-dimensional Gierer-Meinhardt model*, J. Nonlinear Sci., **13**(2), pp. 209–264.

[36] M. J. Ward and J. Wei (2002), *The existence and stability of asymmetric spike patterns in the Schnakenburg model*, Studies in Appl. Math., **109**(3), pp. 229–264.

[37] M. J. Ward and J. Wei (2002), *Asymmetric spike patterns for the one-dimensional Gierer-Meinhardt model: equilibria and stability*, Europ. J. Appl. Math., **13**(3), (2002), pp. 283–320.

[38] M. J. Ward and J. Wei (2003), *Hopf bifurcation of spike solutions for the shadow Gierer-Meinhardt model*, Europ. J. Appl. Math., **14**(6), pp. 677–711.

[39] J. Wei and M. Winter (2001), *Spikes for the two-dimensional Gierer-Meinhardt system: the weak coupling case*, J. Nonlinear Sci., **11**(6), pp. 415–458.

[40] J. Wei and M. Winter (2002), *Spikes for the two-dimensional Gierer-Meinhardt system: the strong coupling case*, J. Diff. Eq., **178**, pp. 478–518.

[41] J. Wei and M. Winter (2003), *Existence and stability of multiple spot solutions for the Gray-Scott model in* $\mathbb{R}^2$, Physica D., **176**(3-4), pp. 147-180.
[42] J. Wei and M. Winter (2008), *Stationary multiple spots for reaction-diffusion systems*, J. Math. Biol., **57**(1), pp. 53–89.
[43] J. Wei and M. Winter (2004), *Existence and stability analysis of asymmetric patterns for the Gierer-Meinhardt system*, J. Math. Pures Appl. (9), **83**(4), pp. 433-476.
[44] J. Wei and M. Winter (2003), *Asymmetric spotty patterns for the Gray-Scott model in* $\mathbb{R}^2$, Studies in Appl. Math., **110**(1), pp. 63–102.
[45] J. Wei and L. Zhang (1998), *On a nonlocal eigenvalue problem*, Ann. Sc. Norm. Sup. Pisa C1. Sci. pp. 41–62.
[46] J. Wei (2008), *Existence and stability of spikes for the Gierer-Meinhardt system*, book chapter in *Handbook of Differential Equations, Stationary Partial Differential Equations*, Vol. 5 (M. Chipot ed.), Elsevier, pp. 489–581.